3-1999

Using the WSR-88D to Forecast Downburst Winds at Cape Canaveral Air Station and the Kennedy Space Center (CCAS/KSC)

Gerald D. Sullivan Jr.

USING THE WSR-88D TO FORECAST DOWNBURST WINDS AT CAPE CANAVERAL AIR STATION AND THE KENNEDY SPACE CENTER (CCAS/KSC)

THESIS

Gerald D. Sullivan, Jr., First Lieutenant, USAF

AFIT/GM/ENP/99M-12

DEPARTMENT OF THE AIR FORCE
AIR UNIVERSITY
AIR FORCE INSTITUTE OF TECHNOLOGY

Wright-Patterson Air Force Base, Ohio

AFIT/GM/ENP/99M-12

USING THE WSR-88D TO FORECAST DOWNBURST WINDS AT CAPE CANAVERAL AIR STATION AND THE KENNEDY SPACE CENTER (CCAS/KSC)

THESIS

Presented to the Faculty of the Graduate School of Engineering

of the Air Force Institute of Technology

Air University

Air Education and Training Command

In Partial Fulfillment of the

Requirements for the Degree of

Master of Science in Meteorology

Gerald D. Sullivan, Jr. , B.S.

First Lieutenant, USAF

March, 1999

AFIT/GM/ENP/99M-12

USING THE WSR-88D TO FORECAST DOWNBURST WINDS AT CAPE CANAVERAL AIR STATION AND THE KENNEDY SPACE CENTER (CCAS/KSC)

Gerald D. Sullivan, Jr., B.S.
First Lieutenant, USAF

Approved:

Lt Col Michael K. Walters Chair, Advisory Committee	1 Mar 99 Date
Lt Col Cecilia A. Miner Member, Advisory Committee	1 Mar 99 Date
Dr. David Weeks Member, Advisory Committee	1 Mar 99 Date
Professor Daniel E. Reynolds Member, Advisory Committee	1 Mar 99 Date

The views expressed in this thesis are those of the author and do not reflect the official policy or position of the Department of Defense of the U. S. Government

Acknowledgements

There were many people to whom I am indebted; to list them all would be impossible. I would like to specifically mention those who deserve special acknowledgements. Firstly, I would like to express my appreciation to my thesis advisor, Lt Col Mike Walters, for his advice and guidance throughout this research. I would also like to thank MSgt Pete Rahe for his expertise with the UNIX system. Without his help, this thesis could not have been accomplished.

Miss Karen Cooper at the National Severe Storms Laboratory deserves many thanks for the numerous times she answered questions and researched problems regarding WATADS.

I thank my children, Kenneth and Jesika, for giving me the inspiration to achieve this goal. Most importantly, I thank God for giving me the strength and perseverance to complete this project.

Gerald D. Sullivan, Jr.

Table of Contents

List of Figures

List of Tables

Abstract

The 45 Weather Squadron (WS) is tasked with providing several convective wind warnings in support of the U. S. Space Program. The forecasters use a radar-based forecast technique to determine if a thunderstorm has the potential to produce a gust that meets warning criteria. This technique, the Echo Top/Vertically Integrated Liquid Wind Gust Potential (ET/VIL WGP), has not previously been evaluated for use in the Cape Canaveral Air Station and Kennedy Space Center (CCAS/KSC) locale. Additionally, there are two other radar-based forecast techniques that required evaluation for possible inclusion into the 45 WS forecast process. These are the Maximum Reflectivity/ Height of Maximum Reflectivity (d/H) Wind Gust Potential and the Storm Top/Vertically Integrated Liquid (ST/VIL) Wind Gust Potential techniques.

Radar data from 15 pulse-type storms that occurred in the CCAS/KSC locale were collected. Potential wind gust forecasts were calculated using the techniques mentioned above. The forecast and observed wind gusts were analyzed using visual and numerical tools to assess the performance of the WGP techniques.

Results of the research indicated that the WGP techniques could not consistently predict the magnitude of the downburst gust. The average errors of the prediction were on the order of 10 knots and were quite variable. Because of the small sample size, these results cannot be considered as conclusive; however, they may indicate that these techniques do not display the degree of accuracy required to be used operationally by the 45 WS.

USING THE WSR-88D TO FORECAST DOWNBURST WINDS AT CAPE CANAVERAL AIR STATION AND THE KENNEDY SPACE CENTER (CCAS/KSC)

1. Introduction

1.1 Background

On 16 Aug 94 a severe thunderstorm event which produced 65-knot wind gusts occurred at the KSC Shuttle Landing Facility (SLF). These gusts were much higher than forecast and thus prompted, over the following years, the development of several techniques for the forecasters of the 45th Weather Squadron (45 WS) to use in predicting downburst winds greater than 35 knots (Wheeler, 1994).

A downburst, as defined by Dr. T. Theodore Fujita, is "a strong downdraft that induces an outburst of damaging wind on or near the surface." Fujita further classified downbursts into two scales: macrobursts and microbursts. A macroburst is a downburst that extends to an area greater than 4 km while a microburst extends to an area less than 4 km (Fujita, 1985:8). Because of operational forecast requirements, the 45 WS is mostly concerned with thunderstorms which create downburst winds greater than or equal to 35 knots, regardless of size or occurrence of damage. For this reason, this research is focused on such events. Furthermore, the reader is advised that the terms downburst and microburst may be use interchangeably to describe these events within the scope of this thesis.

Currently, the 45 WS uses a conceptual forecast model, the "Microburst Funnel", to aid in the forecasting of microbursts (Figure 1). This model guides the forecaster through various steps of the forecast process. First, using outlook techniques 6-10 hours prior to threatening weather, the forecasters determine if the atmosphere is conducive to microbursts. As time passes, the forecasters use intermediate techniques such as interpretation of satellite imagery to determine if thunderstorms are imminent. Finally, nowcasting techniques are used up to 30 minutes prior to the event to finalize the forecast before the warning is issued. These nowcasting techniques include the use of the Weather Surveillance Radar 88 Doppler (WSR-88D) to determine if a thunderstorm has the potential of producing strong downburst winds.

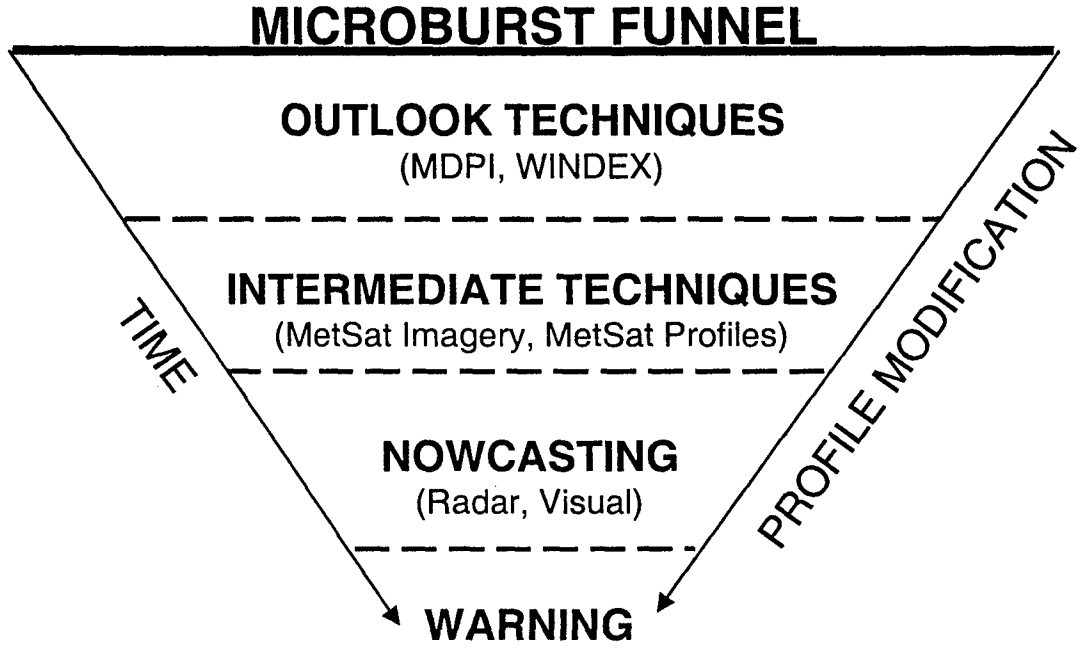

Figure 1. Microburst Funnel (Adapted from Roeder, 1998b:2)

To determine if a storm cell has the potential to produce a threatening downburst, the forecasters use a technique developed by Dr. Stacy Stewart of the National Weather

Service (NWS) and later modified by meteorologists at the Air Force's Air Weather Service (AWS) (Stewart, 1991:5; AWS, 1996:7). This technique uses the Echo Top (ET) and Vertically Integrated Liquid (VIL) values produced by the WSR-88D algorithms to calculate the wind gust potential (WGP) of the storm (Figure 2). The ET is the height of the highest 18.5 dBZ reflectivity value. To achieve the Final Wind Gust Potential (FWGP), the forecaster must add an environmental wind correction. This correction factor is all or a fraction of the mean surface to 5,000-feet wind. (The exact correction factor has been determined to be location-dependent and will be evaluated in this research.)

Wind Gust Potential (WGP) Chart

VIL (kg/m^2)

ET	15	20	25	30	35	40	45	50	55	60	65	70
60								10	16	23	29	34
55							12	21	27	32	36	40
50					9	16	24	30	34	38	42	45
45				10	20	26	31	36	40	43	46	49
40		9	15	21	27	32	36	40	43	47	50	53
35	13	18	23	27	32	36	41	43	47	50	53	56
30	18	23	28	32	36	40	43	47	49	53	56	58
25	23	28	32	36	41	44	47	49	52	55	57	59
20	26	31	36	40	44	48	50	52	55	56	59	60
15	29	34	38	43	47	50	53	55	56	58	61	61

VIL value in **kg/m^2**
Echo Tops in **thousands of feet**
WGP in **knots**

SFC-5,000 ft mean speed = environmental flow
Max Gust = WGP + environmental flow

Figure 2. ET/VIL Wind Gust Potential, (AWS, 1996)

In addition to the ET/VIL WGP technique, Stewart has proposed two other techniques for predicting wind gust potential. The first is the Maximum Reflectivity / Height of Maximum Reflectivity technique (d/H) (Stewart, 1996:325). With this technique, the forecaster uses the WSR-88D to determine the maximum reflectivity of a storm and the height of that reflectivity value. These two values are then used to calculate the wind gust potential. The second technique is the Storm Top / Vertically Integrated Liquid Wind Gust Potential (ST/VIL WGP) technique (Roeder, 1998a). This technique is similar to the ET/ VIL WGP technique except it uses the value of the Storm Top (ST) in place of the ET. The 45 WS does not currently use either of the d/H or ST/VIL WGP techniques. Furthermore, no formal study of the ST/VIL WGP technique has been performed.

It should be noted that these three techniques are designed to predict the maximum potential speed of a downburst not the occurrence of a downburst.

1.2 Problem Statement

The ET/VIL, ST/VIL, and d/H Wind Gust Potential techniques require performance assessments for the Cape Canaveral Air Station and Kennedy Space Center locale.

1.3 Objective

This thesis seeks to provide the 45 WS with an assessment of the performance of the three wind gust potential techniques mentioned above. Additionally, a comparison of the performances of the three techniques will be accomplished.

1.4 Importance of Research

The 45 WS provides tailored prelaunch and launch weather support to Department of Defense, National Aeronautics and Space Administration, and commercial users of the Eastern Range, including CCAS and KCS. This support provides protection for over 25,000 personnel and over $8 billion worth of resources, not including launch vehicles and payload. Although launches are the most visible aspect of operations, there are numerous ground activities (e.g., transporting and erecting vehicles and payloads; moving of solid rocket motors; and fueling/defueling operations) which can also be adversely impacted by strong wind gusts.

Location	Criterion	Lead-time
KSC (Sfc-300 ft)	≥ 35 knots	30 min
	≥ 50 knots	60 min
	≥ 60 knots	60 min
CCAS (Sfc-200 ft)	≥ 35 knots	30 min
	≥ 50 knots	60 min
PAFB (Sfc)	≥ 35 knots	60 min
	≥ 50 knots	60 min
Melbourne	≥ 50 knots	Observed

Table 1. 45 WS Convective Wind Warning Criteria

The 45 WS is tasked with issuing the various convective wind warnings shown in Table 1. These warnings are meant to provide personnel with adequate time to prepare for adverse weather. Lack of preparation may result in the loss of property and even loss of life. The ability to accurately predict the wind gust potential of a storm cell would be invaluable to the forecaster in order to meet these warning requirements.

1.5 Overall Approach

There were six steps accomplished during this research. The first step was to determine days that were potential candidates for the study. A concurrent microburst climatology study at Texas A&M University indicated 57 potential microbursts days. One other day identified by the Applied Meteorology Unit (AMU) at KSC was added to this data set for a total of 58 days.

Days on which there was significant synoptic forcing, a thermodynamic profile uncharacteristic of microbursts, or no data available were eliminated, leaving 11 days. On these 11 days, 15 thunderstorms were identified as producing convective downburst winds, i.e., a microburst.

Wind sensor data from the CCAS/KSC Weather Information Network Display System (WINDS) were then sorted to identify times of potential events. The WINDS system consists of 44 instrument towers positioned throughout the CCAS/KCS complex (Figure 3).

The Archive Level II radar data for times surrounding these events were analyzed using the WSR-88D Algorithm Testing and Display System (WATADS) Version 10.0. The required parameters were collected and forecast winds were calculated using each of the three wind gust potential techniques.

The predicted values were then compared to the gust values recorded by the WINDS network and statistical values were calculated to achieve a measure of each technique's performance when compared to the observed gusts.

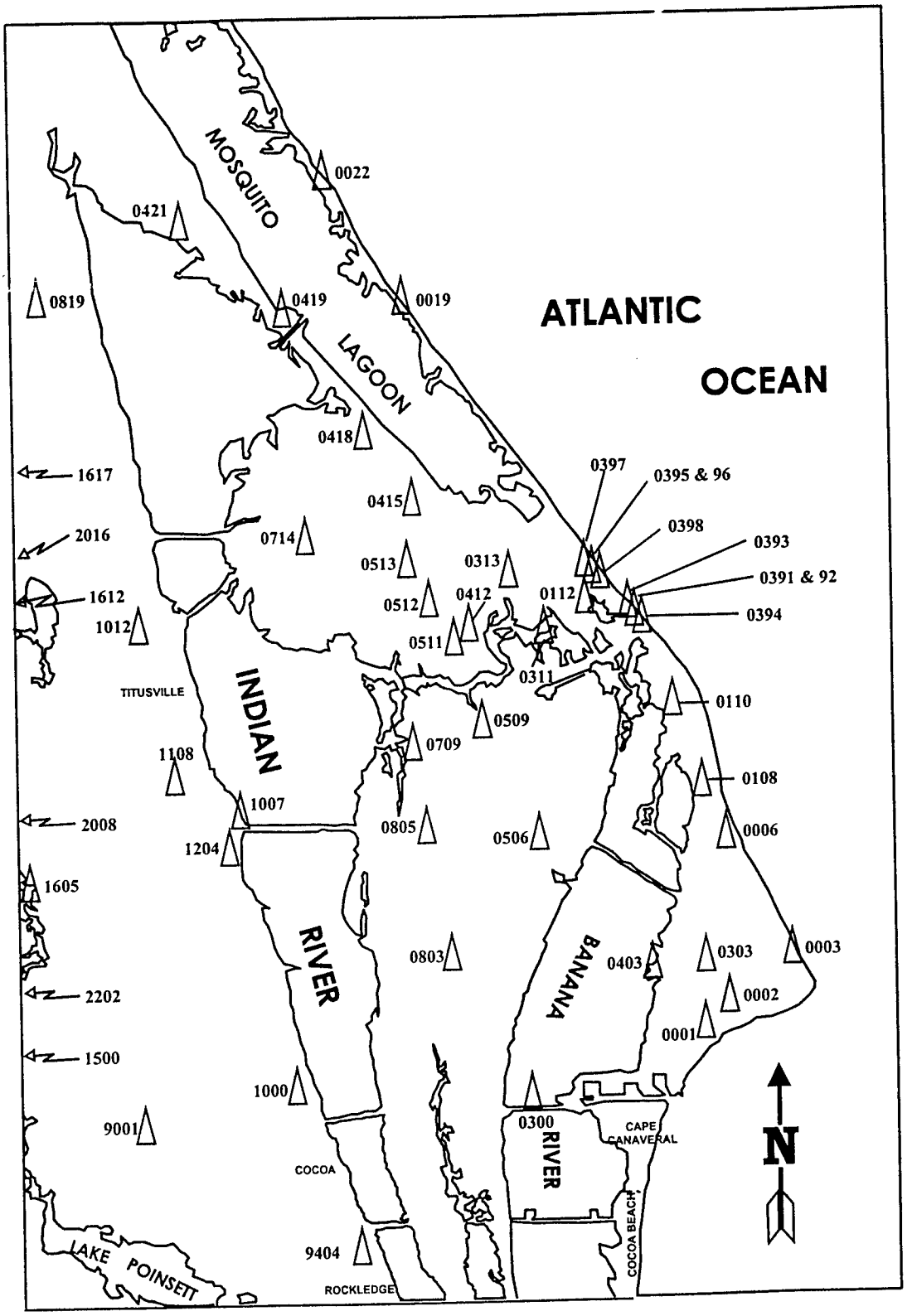

Figure 3. Map of WINDS Network (Adapted from Roeder, 1998b:1)

1.6 Organizational Overview

Chapter 2 presents a review of literature regarding convective downbursts and microbursts and past studies using the wind gust potential techniques. The theory in which these techniques are founded is discussed briefly. Some radar theory is also included to ensure the reader understands the WSR-88D's functions and limitations. Chapter 3 covers the methodology used during the data gathering process and fully describes each step. Also included is information on WATADS and its limitations. Chapter 4 describes the data collection and analysis under various situations. Chapter 5 is a summary of the results and conclusions, along with suggestions for further research.

2. Literature Review

2.1 Downbursts

During an aerial survey of damage created by the superoutbreak of tornadoes on 3-4 April 1974, Dr. T. Theodore Fujita noticed a damage pattern unlike that created by the swirling air of tornadoes. Instead, hundreds of trees were blown down in a starburst pattern similar to that created by a garden hose when sprayed on the ground. Fujita postulated that this damage was the product of an intense downdraft that spread out in a fan-shaped fashion after impacting the ground. Then after thorough investigation of the Eastern 66 aircraft accident at John F. Kennedy Airport on 24 June 1975, Fujita hypothesized that such a strong downdraft caused the crash and named this phenomenon a "downburst" (Fujita, 1985:1-2).

Fujita's contemporaries did not readily accept his concept of a downburst, defined as a strong downdraft inducing strong, possibly damaging surface winds. Most meteorologists believed that a downdraft should weaken considerably below cloud level and thus be insignificant upon reaching the ground. Over the next decade, Fujita took part in several studies to settle the controversy. Two of the important projects that helped Fujita prove his concept were the Northern Illinois Meteorological Research On Downbursts (NIMROD) and the Joint Airport Weather Studies (JAWS) (Fujita, 1985:2).

2.1.1 NIMROD

Conducted by Fujita and Srivastava in 1978, NIMROD was the first project designed to study downbursts. Located in the western suburbs of Chicago, the project network consisted of three Doppler radars and 27 Portable Automated Mesonet (PAM)

stations. During the 42-day project, Fujita observed a large number of downbursts. Based on his observations, Fujita further classified downbursts into two subcategories, macrobursts and microbursts, based on the horizontal extent of the winds. Macrobursts are large downbursts that have horizontal extents greater than 4 km. Microbursts are those with horizontal extents less than 4 km. Of the 50 microbursts observed, 64% were associated with measurable rain at the surface. This lead to a further classification of microbursts into "wet" microbursts and "dry" microbursts, depending on the associated rainfall (Fujita, 1985: 4-6).

2.1.2 JAWS

In 1982, the University of Chicago and the National Center for Atmospheric Research jointly conducted the JAWS. Again, Fujita acted as one of the principal investigators. Based in the northern suburbs of Denver, JAWS was designed to study the smaller microburst phenomena because of the growing number of recognized microburst-related aircraft incidents throughout the world. Lasting for 86 days, the JAWS project observed 186 microburst events. Of these events, 155 were dry microbursts. This brought attention to the fact that strong downburst winds can be created by seemingly unthreatening clouds (Fujita, 1985:5).

2.1.3 Characteristics of Microbursts

Following the NIMROD and JAWS projects, Fujita was able to differentiate between the two types of microbursts previously identified: the wet microburst and the dry microburst. Wet microbursts are most likely to occur in regions where there is ample moisture available. There is a shallow sub-cloud layer and a measureable amount (0.01 inches or more) of rain is observed at the surface. Dry microbursts, on the other hand,

mostly occur in arid regions and originate in high-based clouds. Any precipitation evaporates below the cloud before reaching the surface. Due to the ample moisture, mostly wet microbursts occur on the Florida peninsula.

2.1.4 Environmental Conditions Conducive for Wet Microbursts

In 1991, Atkins and Wakimoto performed a thorough analysis of the thermodynamic properties of the wet microburst producing days observed during the 1986 Microburst and Severe Thunderstorm (MIST) project conducted in northern Alabama. The most significant finding of this analysis was that the equivalent potential temperature (θ_e) profile could play an important role in determining if microbursts are likely to occur that day. They found on days that microbursts occurred, the difference between the near-surface θ_e and the minimum θ_e aloft ($\Delta\theta_e$) was greater the 20 K. The $\Delta\theta_e$ on non-microburst producing days was less than 13 K. Atkins and Wakimoto propose that there is $\Delta\theta_e$ threshold between 13 and 20 K that could distinguish between microburst and non-microburst days (Atkins and Wakimoto, 1991:472-4).

Equivalent potential temperature is defined as the temperature an air parcel would have after undergoing dry-adiabatic expansion until saturated, pseudo-adiabatic expansion until all moisture is precipitated out, and finally dry-adiabatic compression to 1000 hPa. This temperature is conservative with respect to dry and pseudo-adiabatic processes (Huschke, 1959:208).

The mathematical equation for equivalent potential temperature is:

$$\theta_e = T_e \left(\frac{p_o}{p} \right)^{\frac{R}{c_p}} , \quad (1)$$

where

$$T_e = T \exp \frac{Lw}{c_p T} \quad (2)$$

and

θ_e is the equivalent potential temperature (Kelvin),

T_e is the equivalent temperature (Kelvin),

p is pressure at which T_e is measured (hPa),

p_o is reference pressure of 1000 hPa,

R is the gas constant for dry air (287 J K^{-1} kg^{-1}),

c_p is the specific heat of air at constant pressure (1004 J K^{-1} kg^{-1}),

L is the latent heat of evaporation (2.25 x 10^6 J kg^{-1}),

w is the mixing ration (kg kg^{-1}).

The existence of low θ_e air aloft is important because the dry, cold air provides an atmosphere that is favorable for evaporative cooling and thus aids in the generation of negative buoyancy. This negative buoyancy is believed to be a key factor in the development of microbursts. Current research has shown that a minimum θ_e of at least 333 K is necessary to create the proper environmental conditions (Stewart, 1998).

2.2 Downburst Gust Prediction Techniques

Building on the work of Squires and Paluch, Emanuel (1981) developed a similarity theory to describe penetrative plumes and thermals and applied the theory to downdrafts. Using a system of conservation equations for the total time rate of change of mass, momentum, heat and water deficit, Emanuel showed the vertical velocity of a penetrative thermal is given by

$$w^2 = -\tfrac{1}{2}\alpha F_0 z^{-2} - \tfrac{2}{7}(M - g)l_c z - \tfrac{1}{16}N^2 z^2, \qquad (3)$$

where

w is the vertical velocity (m s^{-1}),

α is a the entrainment constant (unitless),

F_0 is the boundary condition for buoyancy flux (m^4 s^{-2}),

z is the penetrative depth (m),

M is a latent heat constant (m s^{-2}),

g is acceleration due to gravity (m s^{-2}),

l_c is cloud liquid water mixing ratio (g kg^{-1}),

N is a Brunt-Väisälä frequency (s^{-1}).

Following Emanuel, equation (3) may be simplified by using values for M and N^2 that are typical of a cloud in a tropical atmosphere. These values are M = 82 m s^{-2} and N^2= 5 x 10^{-5} s^{-2} (Emanuel, 1981:1548-9). This results in the following equation:

$$w^2 = -20.628571 ms^{-2} l_c z - 3.125 \times 10^{-6} s^{-2} z^2 \qquad (4)$$

This equation may be used to calculate the vertical velocity of a downdraft given the cloud liquid water content, l_c, and height at which the downdraft initiates, z.

2.2.1 ET/VIL Potential Gust Technique

Since directly measuring cloud liquid water content is not feasible, it is normally estimated by means of indirect remote sensing with microwave radar. The radar reflectivity factor, z_r, may then be used to estimate the liquid water content by using the following equation:

$$l_z = 3.44 \times 10^{-3} z_r^{4/7}, \tag{5}$$

where l_z is the radar derived liquid water content (g m^{-3}) and z_r is the radar reflectivity factor (mm^6 m^{-3}). Integrating (5) vertically over a geographic area provides an estimate of the liquid water content in the column above that area. This estimate is called the Vertically Integrated Liquid (VIL) (Greene and Clark, 1972).

In an attempt to estimate the independent variables of (4), Stewart substituted the average rainwater content, R_c (kg m^{-3}), for l_c and ET for z. R_c is obtained by dividing VIL by the ET. In order to convert R_c to the proper units (g g^{-1}) it is assumed that 1 kg of dry air is equal to 1 m^{-3} in volume, the approximate density of dry air at 700 hPa. This results in the following equation:

$$w = \left[(20.628571 VIL) - \left(3.125 \times 10^{-6} ET^2\right)\right]^{1/2}, \tag{6}$$

where w is the downward vertical velocity of the downdraft in m s^{-1} (Stewart,1991,1992,1996). Equation (6) can be used to construct Table 2. A three-dimensional plot of the surface created by equation (6) is shown in Figure 4.

ET (kft) \ VIL (kg m^{-2})	15	20	25	30	35	40	45	50	55	60	65	70
60									18	27	33	39
55							14	24	31	37	42	46
50						19	28	34	39	44	48	52
45				11	22	30	36	41	45	49	53	57
40			14	24	31	37	42	46	50	54	57	61
35		15	25	31	37	42	46	50	54	58	61	64
30	13	24	31	37	42	46	50	54	57	61	64	67
25	22	29	35	41	45	49	53	57	60	63	66	69
20	27	33	39	43	48	52	55	59	62	65	68	71
15	30	36	41	46	50	53	57	60	63	66	69	72

Table 2. Stewart's ET/VIL Potential Wind Gust (kts) Table

Upon verification of this technique, Stewart found that a correction factor of 1/3 of the mean surface-to-5,000 foot wind must be added to the wind gust prediction to obtain a final gust prediction (Stewart, 1991:16). Further verification of the technique by Frazier suggested that the entire mean wind value should be added (Frazier, 1994). Stewart and Frazier conducted these studies using WSR-57 RADAP-II data which has a coarser resolution, 3X5 nm, as opposed to the WSR-88D, with a 2.2 x 2.2 nm resolution. As a result, further study is required to determine the appropriate correction factor since the WSR-88D is the system in current use by NWS and DoD weather stations.

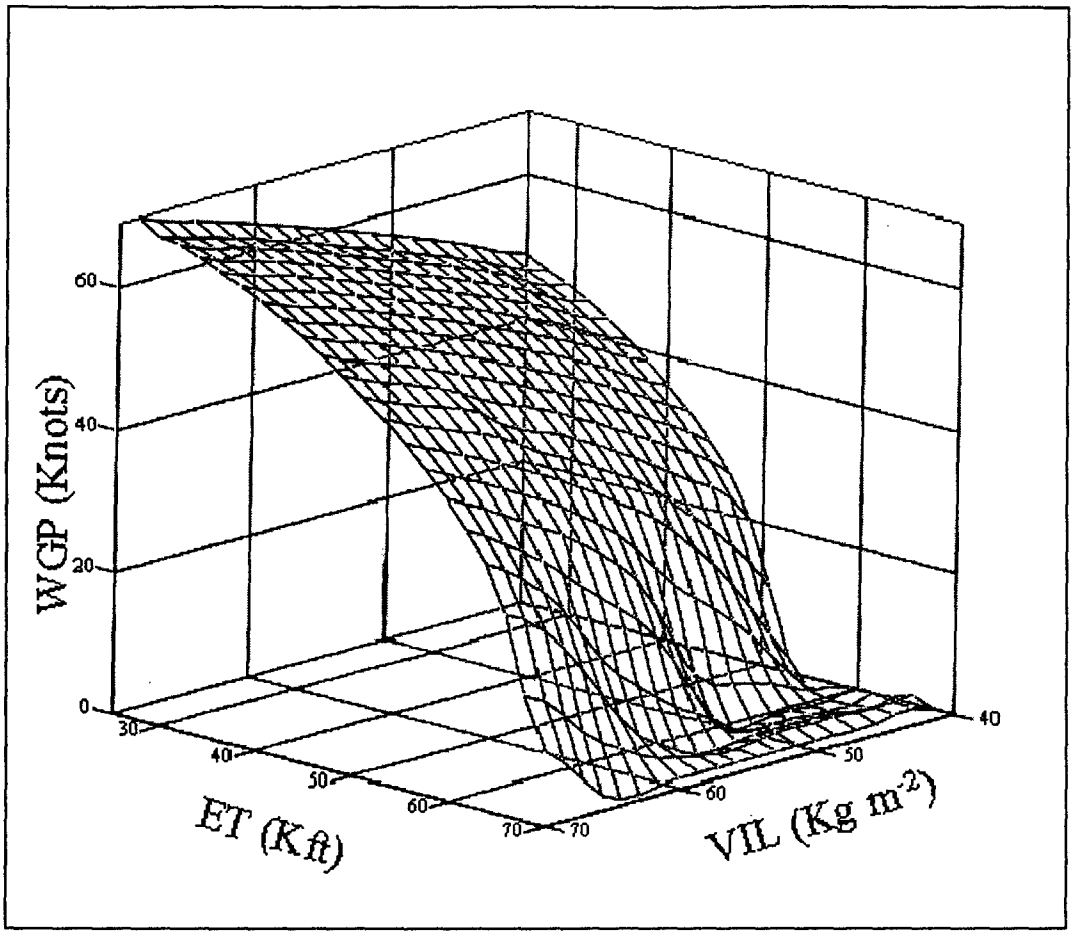

Figure 4. WGP Equation Surface Plot

This figure is a three-dimensional representation of equation 6. The rippling in the lower right is an artifact of the interpolation scheme. The actual values in this region are imaginary.

2.2.2 dBZ/Height (d/H) Potential Gust Technique

Another technique developed by Stewart takes advantage of the technological advances applied in development of the WSR-88D system. Users of the WSR-88D have the ability to determine the maximum reflectivity factor, z_r, of a storm cell and the height, H, at which the maximum reflectivity occurs. Substitution of l_z for l_c and H for z in (4) yields the following equation which may also be used to predict potential wind gusts:

$$w = \left[(20.628571 l_z H) - (3.125 \times 10^{-6} H^2\right]^{1/2}. \quad (7)$$

Unlike the ET/VIL technique, the d/H technique does not require the addition of a correction factor. This equation can be used to create a nomogram (Figure 5) for graphical calculation of wind gust potential. To obtain the WGP, the user follows a vertical line from the height of the maximum reflectivity until it intersects with the corresponding maximum reflectivity curve. Then the WGP can be found by following a horizontal until it intersects vertical axis.

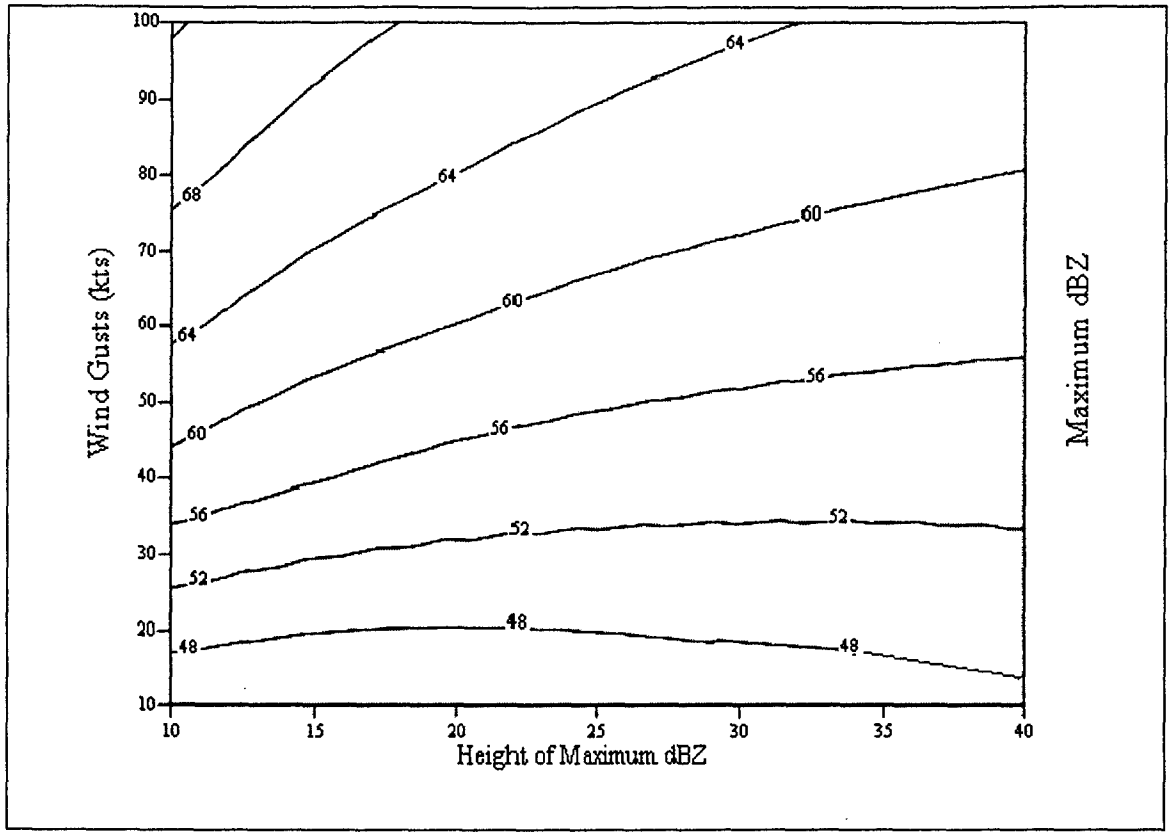

Figure 5. d/H Nomogram

2.2.3 ST/VIL Wind Gust Potential

Another method for predicting wind gust potential has been proposed by Stewart (Roeder, 1998; Stewart, 1998). This technique is similar to the ET/VIL technique except the Storm Top (ST), the height of the highest 30-dBZ reflectivity value, is substituted for the ET. There have been no formal studies of this technique to date.

2.2.4 AWS ET/VIL WGP Table

In 1996, Air Weather Service (AWS) published an issue of ECHOES, a series of publications aimed at enhancing the use of radar, entitled "Operational Use of Vertically Integrated Liquid (VIL)." In this issue, the authors describe using the ET/VIL technique as a means for predicting downburst potential (AWS, 1996). The table published was

shown as Figure 2. Stewart's 1991 paper was cited as the source of the table, however, comparison of the AWS table and Stewart's (Table 2) shows that the two are not the same. The following table illustrates the difference between the two tables.

ET (kft) \ VIL (kg m^{-2})	15	20	25	30	35	40	45	50	55	60	65	70
60								**10**	-2	-4	-4	-5
55							-2	-3	-4	-5	-6	-6
50					**9**	-3	-4	-4	-5	-6	-6	-7
45				-1	-2	-4	-5	-5	-5	-6	-7	-8
40		**9**	1	-3	-4	-5	-6	-6	-7	-7	-7	-8
35	**13**	3	-2	-4	-5	-6	-5	-7	-7	-8	-8	-8
30	5	-1	-3	-5	-6	-6	-7	-7	-8	-8	-8	-9
25	1	-1	-3	-5	-4	-5	-6	-8	-8	-8	-9	-10
20	-1	-2	-3	-3	-4	-4	-5	-7	-7	-9	-9	-11
15	-1	-2	-3	-3	-3	-3	-4	-5	-7	-8	-8	-11

Table 3. Difference Between AWS ET/VIL Table and Stewart's ET/VIL Table

There are significant differences between the two tables. The bold numbers in Table 3 show where the AWS table had values yet Stewart's table did not. The Air Force Weather Agency (AFWA, formerly AWS) was contacted to determine the justification for the differences; however, no scientific foundation for the change was found. Nevertheless, the 45 WS uses the AWS table as one of it's forecasting tools and is interested in assessing its performance.

2.3 WSR-88D Background (FMH-11)

The Weather Surveillance Radar 88 Doppler (WSR-88D), or NEXRAD as it is known to the general public, is the preeminent weather radar employed by the operational forecasting community. The WSR-88D is an S-band radar that emits an electromagnetic

wave at a specific wavelength (10.7 cm) and power. By comparing the amount of power returned from a target to the emitted power, the WSR-88D is able to give operational meteorologists important information about the meteorological target in question. The WSR-88D is also a coherent radar, meaning it has the capability to discern target velocities by applying the Doppler principle.

2.3.1 Operational Modes

The WSR-88D operates in two modes: Clear Air mode and Precipitation mode. Clear Air mode is used when there is little or no precipitation within the range of the radar. In Clear Air mode the radar employs scan strategies that make it more sensitive to smaller targets. This mode is useful to acquire wind velocity information from non-meteorological targets such as dust. In Precipitation mode, the radar uses scan strategies that optimize its ability to gather information on threatening thunderstorms and other meteorological phenomena.

2.3.2 Volume Coverage Patterns

There are also two volume coverage patterns (VCP) employed in each mode. The VCPs used during Clear Air mode are not relevant to this thesis and are not discussed. Precipitation mode uses VCPs 11 and 21. These VCPs provide better sampling of the vertical structure of the storm, and information is available in a more timely manner than in Clear Air mode. VCP 11 (Figure 6) uses 14 elevation angles and a scan time of 5 minutes providing the better coverage for storms within 60 nm of the radar. VCP 21 (Figure 7) uses 9 elevation angles and a scan time of 6 minutes. This VCP provides better coverage for storms beyond 60 nm due to the slower rotation rate of the radar.

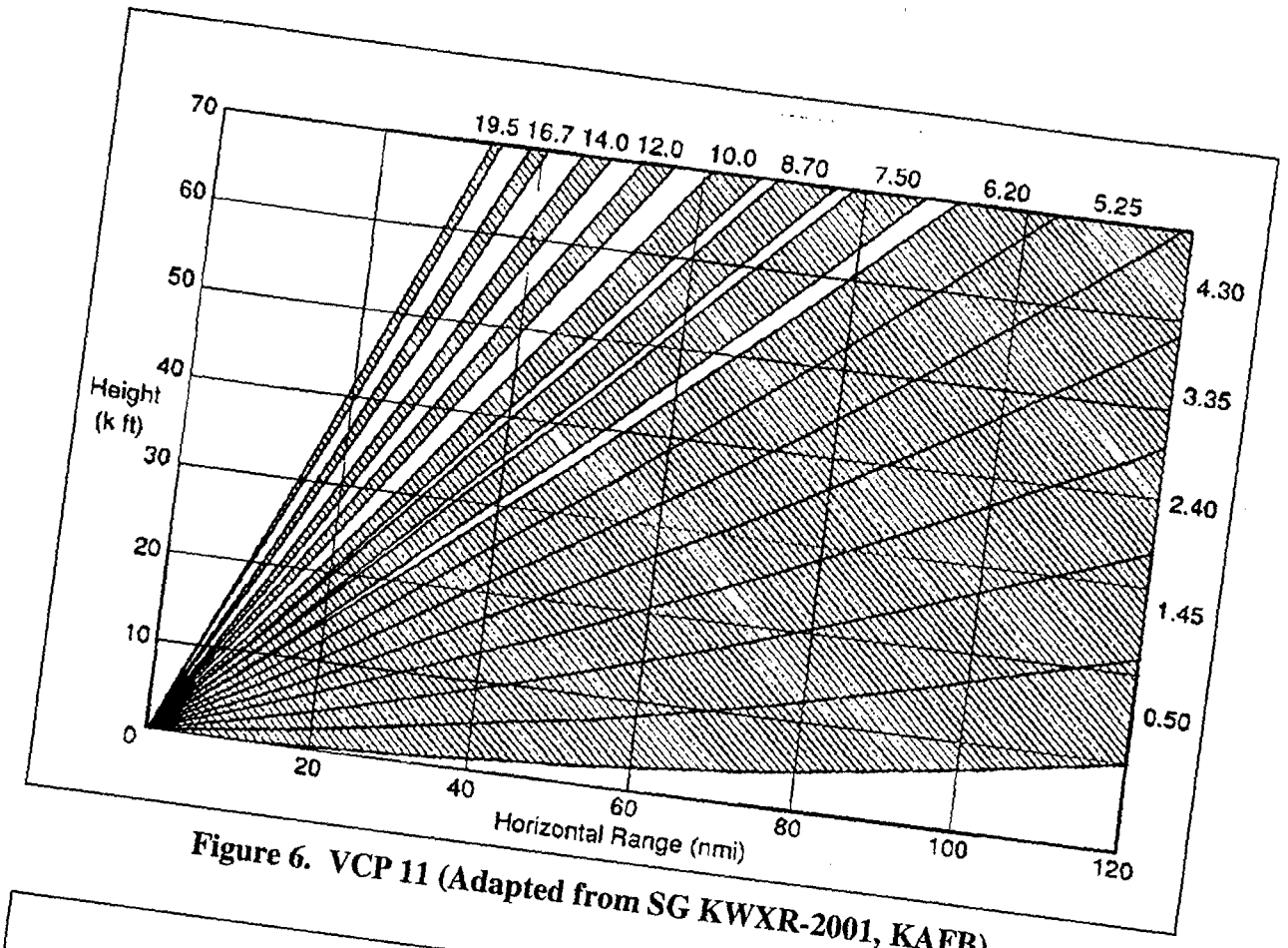

Figure 6. VCP 11 (Adapted from SG KWXR-2001, KAFB)

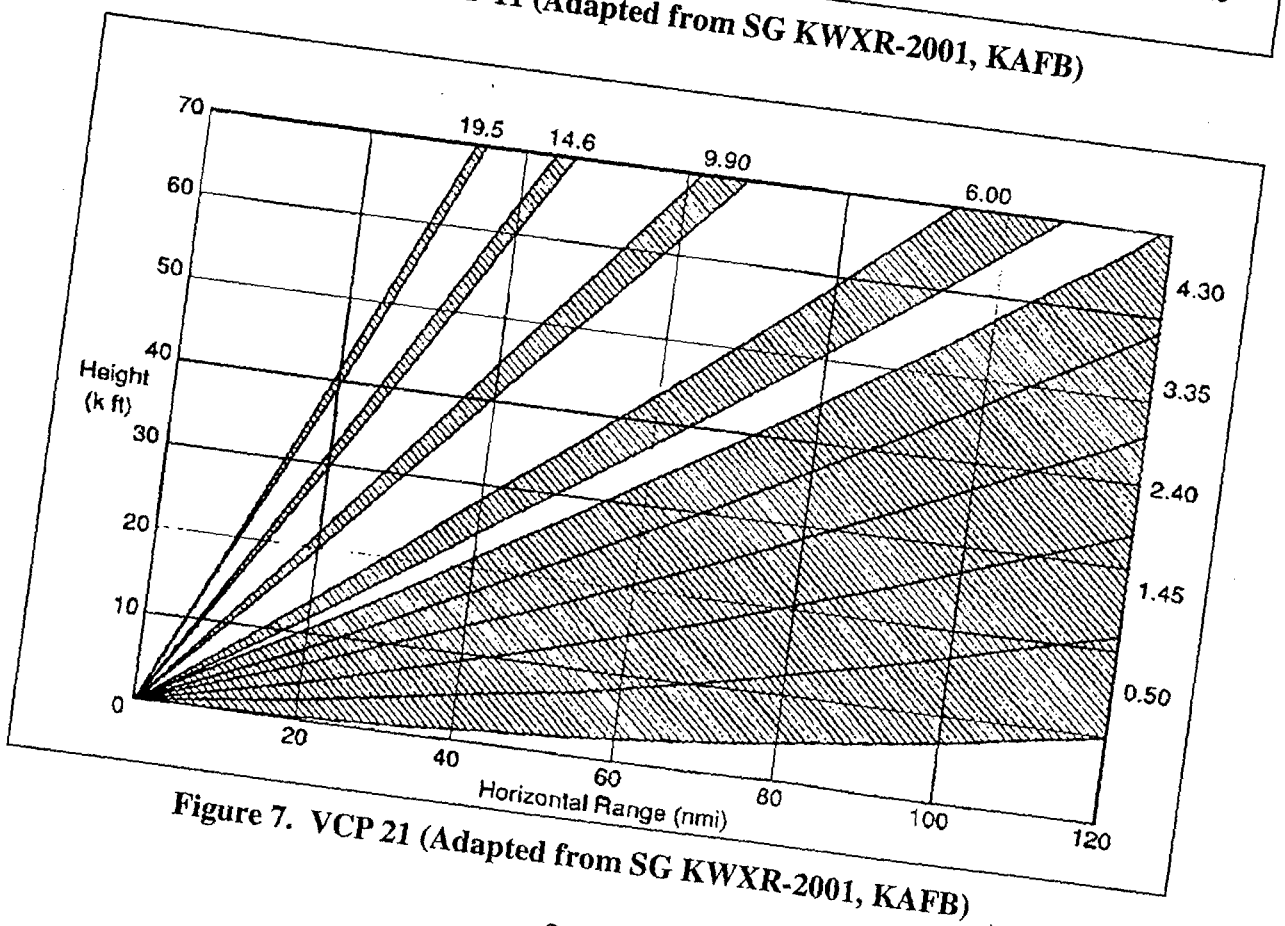

Figure 7. VCP 21 (Adapted from SG KWXR-2001, KAFB)

2.3.3 WSR-88D Products

There are numerous products available at the Principle User Processor (PUP) for the operational forecaster to use while monitoring thunderstorm activity. Three of these products are essential to applying the techniques discussed in this thesis. These are the Echo Top (ET), the Vertically Integrated Liquid (VIL) and the Cell Trends (CT) products.

2.3.3.1 Echo Top (ET) Product

The Echo Top (ET) product is a graphical representation of the height of the highest sample volume meeting the minimum reflectivity value of 18.5 dBZ (Figure 8). The product is updated once per volume scan, every 5-6 minutes depending on VCP, assuming the radar is in precipitation mode. The product has a resolution of 2.2 x 2.2 nm and a range of 124 nm from the radar. It displays heights from 5 to 70 kft in 5 kft bins.

Although the ET product gives a good estimate of the maximum height of the precipitation core, there are several considerations to be aware of during its use. First, there is no correction for contamination from sidelobes. As a result, heights may be overestimated in areas of high reflectivity, such as those due to hail contamination. Also, height overestimation may occur due to beam broadening, giving uniformly high storms a "stair-step" appearance as their range from the radar increases. Finally, underestimation of ET may occur if the actual top lies in one of the vertical gaps between reflectivity slices or if the top of the storm is in the cone of silence, the area above the radar that is beyond the highest elevation angle (Figure 9).

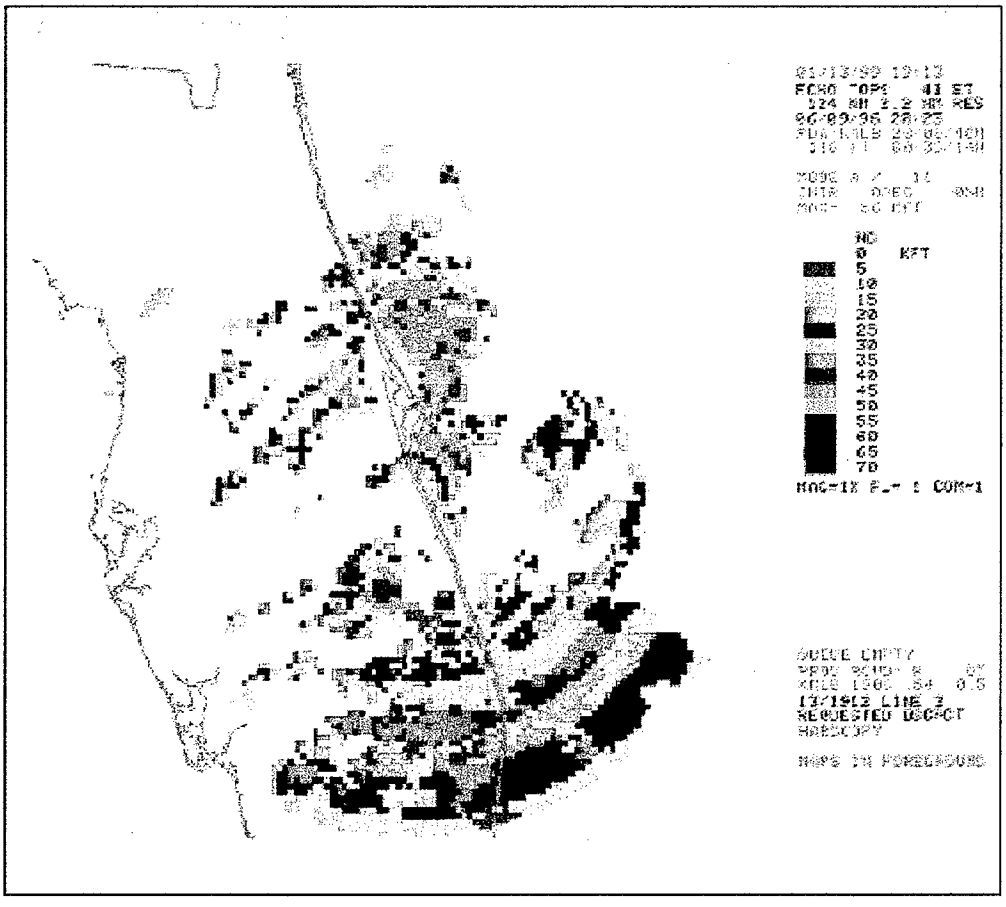

Figure 8. WSR-88D ET Product

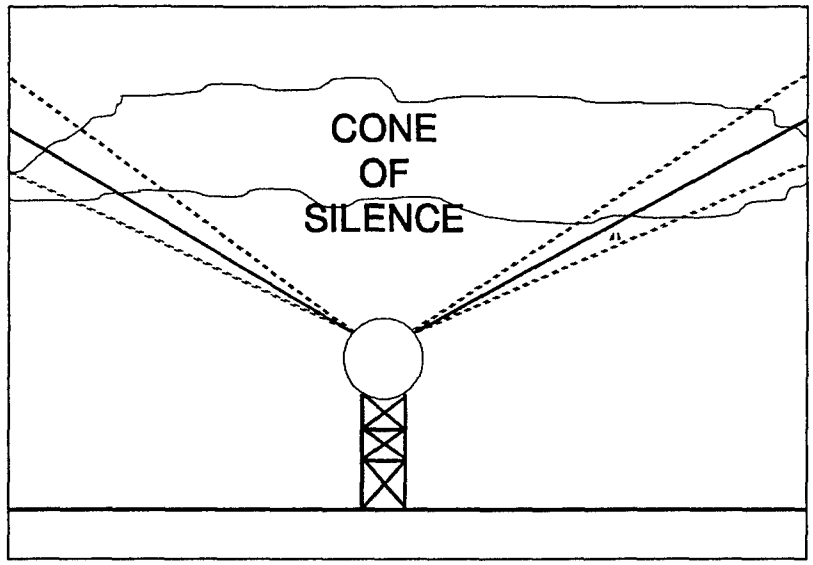

Figure 9. Cone of Silence (Adapted from SG KWXR-2001, KAFB)

2.3.3.2 Vertically Integrated Liquid (VIL) Product

The VIL product is graphical representation of the liquid water in a column above a geographical area (Figure 10). The VIL algorithm uses equation (5) to estimate liquid water content based on theoretical and empirical studies. The VIL product displays VIL values with a 2.2 x 2.2 nm resolution up to a range of 124 nm Values from 0 to 70 kg m^{-2} are displayed in 5 kg m^{-2} bins. The product is updated every 5-6 minutes depending on VCP.

As with the ET product, there are several considerations to be aware of when using the VIL product. Firstly, VIL is a volumetric product meaning it requires the completion of a full volume scan before it can be produced. VIL values for fast moving or strongly tilted storms may be underestimated because their estimates may be assigned to adjacent VIL grid-boxes. Also, underestimation may also occur if the storm is close to the radar, thus being in the cone of silence. Finally, overestimation is possible when

there is large hail present, because the radar is not able to differentiate between liquid water and the highly reflective hailstones. In order to compensate for hail contamination, the VIL algorithm truncates reflectivity values greater than 56 dBZ. This compensation, however, may be counterproductive in areas such as Florida where high reflectivities are possible without hail present.

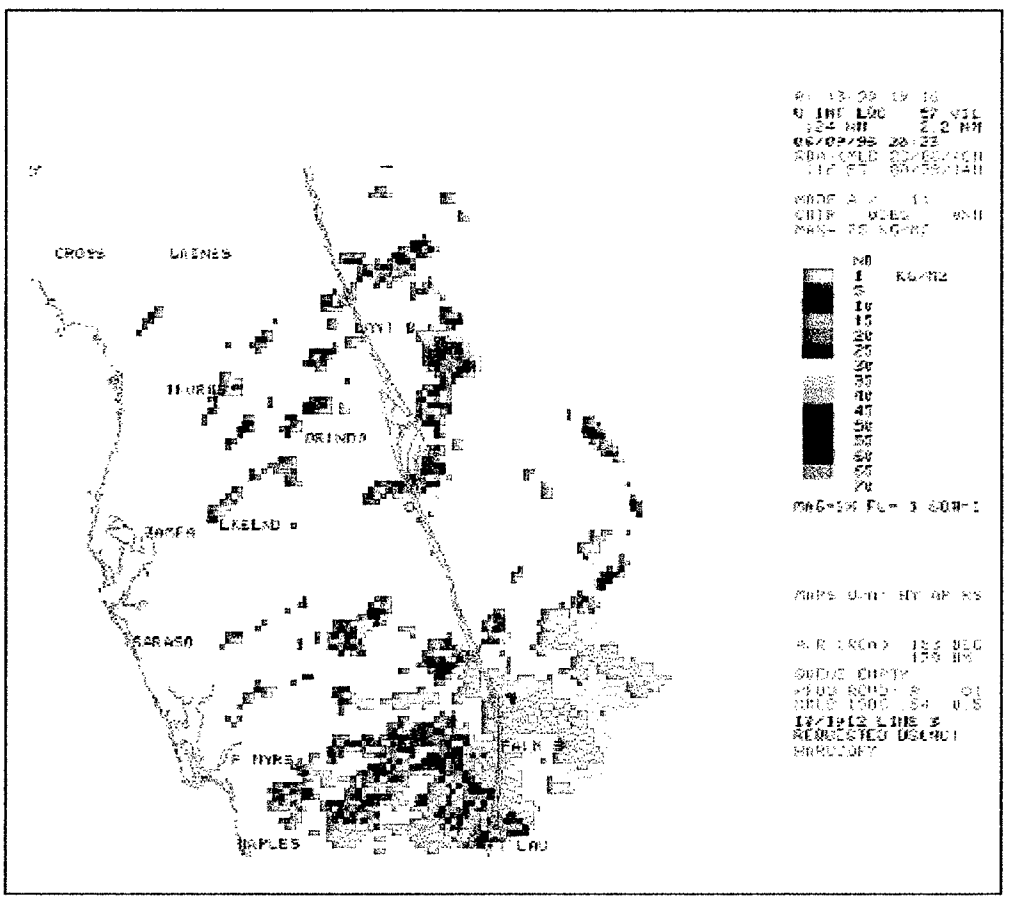

Figure 10. WSR-88D VIL Product

2.3.3.3 Cell Trends Product

The final product pertinent to this thesis is the Cell Trend product. Using this product the operational forecaster can view a time-series of storm parameters for a

specific cell for up to 10 volume scans. Cell Top (Storm Top), Maximum Reflectivity, and Height of Maximum Reflectivity are among the various parameters available. These parameters are used in the d/H and ST/VIL WGP techniques

As with the ET and VIL products, the Cell Trends product may be affected if the storm is within the cone of silence or the VCP in operation does not adequately sample the storm cell.

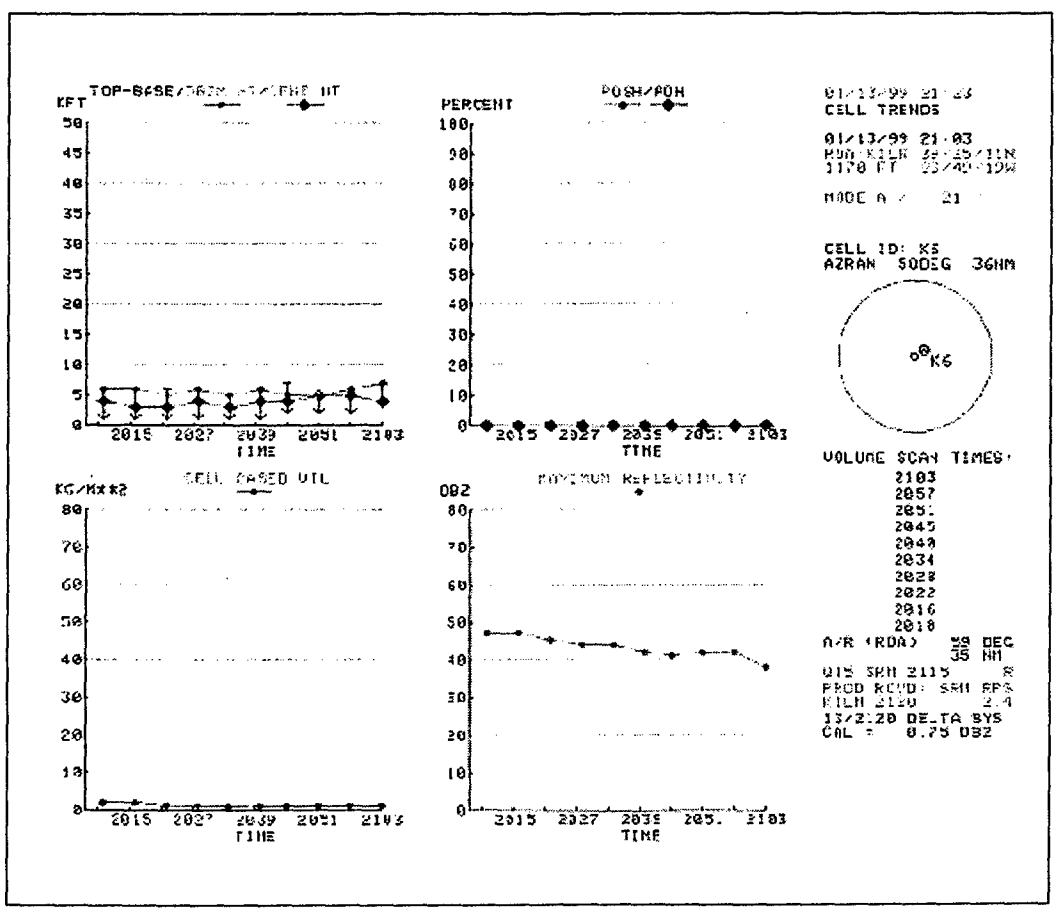

Figure 11. WSR-88D Cell Trends Product

3. Methodology

3.1 Introduction

This thesis seeks to assess the performance of the microburst potential wind gust prediction techniques presented in chapter 2. Microburst events require that certain environmental conditions are met. The methodology presented in this chapter was designed to ensure the data set contained storms which met these conditions as closely as possible.

3.2 Summary of Methodology

The steps taken are summarized as follows:

1) Determine potential days on which a thunderstorm created a wind gust of 35 knots or greater on the CCAS/KSC complex.
2) Verify that the suspect thunderstorms were not synoptically forced.
3) Determine if the equivalent potential temperature profile for the potential day was conducive for producing microbursts.
4) Determine if the event met microburst wind criteria. These criteria were modified from Fujita's criteria to meet the 45 WS requirements (Fujita, 1985:54).
5) Analyze radar data using WATADS 10.0 and collect pertinent parameters.
6) Perform statistical analysis of data acquired in step 5 (presented in chapter 4.)

3.2.1 Determination of Event Days

The preliminary results of a concurrent microburst climatology study of the CCAS/KSC locale being conducted at Texas A&M University identified 57 potential

days during the summer months of 1994 through 1998. One other day identified by the Applied Meteorology Unit (AMU) at Patrick AFB was added to the data set for a total of 58 potential microburst days.

3.2.2 Screening for Synoptic Influence

The techniques being evaluated are designed to predict the maximum potential wind gust of a pulse-type thunderstorm (Stewart, 1991:1). There is little or no synoptic forcing involved in the formation of pulse-type thunderstorms, e.g., a surface front propagating across the Florida peninsula, a tropical storm in the Gulf of Mexico, or significant 500 hPa features.

In order to determine if there were major synoptic features in the CCAS/KSC locale, the National Oceanic and Atmospheric Administration (NOAA) *Daily Weather Maps* for the event days were referenced (NOAA, 1994-1997). It was determined that on 17 of the potential days, there were significant synoptic features that precluded their inclusion in the data set. This left 41 days.

3.2.3 Screening of Thermodynamic Profile

As mentioned in chapter 2, microbursts are most likely to occur on days on which there exists a certain thermodynamic profile. This profile is such that there is a difference of at least 13 K between the surface θ_e value and the minimum θ_e value aloft. There must also be a pocket of low θ_e, less than ~333 K, air in the mid-levels. This low θe air allows the evaporative cooling necessary to produce a microburst once the environmental air is entrained into the thunderstorm.

Cape Canaveral Air Station launches rawinsondes three times per day, at 10, 15 and 22 UTC. The raw data, in ASCII text format, for these soundings were received

from Patrick AFB. Microsoft Excel© was used to reformat the data into a format that could be read by a Mathcad© template that was written to calculate and plot θ_e values (Appendix D). Four of the remaining 41 days did not exhibit the proper thermodynamic profile characteristics leaving 37 possible microburst days.

3.2.4 Screening for Wind Criteria

The wind screening criteria used for the NIMROD and JAWS projects were modified slightly to meet the 45 WS requirements. These modified criteria are:

1) A wind gust greater than or equal to 35 knots.
2) Wind gust greater than or equal to 125% of the three-hour mean wind speed prior to event.
3) Wind gust greater than or equal to 125% of the three-hour mean wind speed after event.
4) Wind gust at least 10 knots greater than three hour mean wind speed prior to event.
5) Wind gust at least 10 knots greater than three hour mean wind speed after event.

The first criterion identifies the events with which the 45 WS is most concerned. The remaining criteria are meant to ensure the wind gust is an isolated event and not synoptically driven. For example, a gust of 35 knots in a wind field that already has a mean speed of 30 knots would not likely be the result of a microburst.

The wind sensor data from the 45 WS WINDS network were received from Patrick AFB in ASCII text format. Microsoft Excel© was used to sort the data. Using the data filter capability, wind gusts of greater than or equal to 35 knots were identified.

Then the average wind speed for the three-hour periods before and after the event was calculated. This step eliminated 8 days because there were no events where there were winds gusts greater than or equal to 35 knots. This left 29 potential days.

3.2.5 Additional Reduction of Event Days

Finally, there were 5 days on which the data necessary to perform the previous steps or the required radar data were not available. This left 24 potential days in the data set.

3.3 Acquisition of Radar Data

The Archive Level II radar data for the potential event days were received from the National Climatic Data Center (NCDC) via a formal request through the Air Force Combat Climatology Center (AFCCC). Archive Level II data are recorded at the Radar Data Acquisition (RDA) unit. It is raw data that may be played back using the WSR-88D Algorithm Testing and Display System (WATADS) version 10.0. WATADS 10.0 can produce most of the WSR-88D products as if real-time.

3.3.1 WATADS

A product of the National Severe Storms Laboratory (NSSL), the WATADS software was created to aid in the development and refinement of the algorithms used by the WSR-88D. For this thesis, the Sun Unix workstation version of WATADS was used. Archive Level II data were received on 8 mm tape and processed by WATADS. After the data is read and processed, nearly all products available to the Principal User Processor (PUP) can be displayed. The PUP is the system by which operational users receive the WSR-88D products in the field.

The only product not readily available using WATADS is the Echo Top product. After consultation with the NSSL, the NSSL Storm Cell Identification and Tracking (SCIT) Algorithm was modified to give an estimate of the Echo Top. In normal operation, the NSSL SCIT output produces the Storm Top (ST), the height of the highest 30 dBZ reflectivity value associated with an identified storm cell. The ST algorithm parameter was changed to 18 dBZ thus giving the height of the highest 18 dBZ reflectivity value, i.e., the ET. Comparison of the WATADS output with two actual WSR-88D ET products for the same times showed that the WATADS ET value was either within the bin displayed by the WSR-88D or was underestimated by one bin level. The bins are lower-bounded 5 kft bins. The implications of this will be discussed in chapter 4.

The radar data for the remaining days were analyzed and the necessary parameters were collected. The parameters and sources are listed in Table 4.

Normal WATADS output:
Time of volume scan
Volume scan number
Volume Coverage Pattern
Grid-based Vertically Integrated Liquid (VIL)
Mean surface-5,000-foot winds (using the VAD wind profile)
WSR-88D SCIT algorithm:
Cell identification number
Azimuth and Range of storm cell
Storm Top
Maximum reflectivity of storm cell
Height of the maximum reflectivity
NSSL SCIT algorithm:
Cell identification number
Echo Top

Table 4. Parameters collected using WATADS

The volume scan used for the VIL techniques was the one that had the highest VIL value before the event. For the d/H technique, the volume scan with the greatest dBZ was used.

During the radar data acquisition process, it was determined that 13 more days needed to be eliminated from the data set. This was due to several reasons, the most common being that the apparent gusts were associated with large storm complexes. This makes discerning which storm cell created the gust very difficult, if not impossible. Another reason for eliminating some days, is that there were no storm cells in the vicinity of the recording tower that could have produced the gust. This left 11 potential microburst days.

Of the 11 potential microburst days, 15 microburst events were identified. The data for these events were collected and will be analyzed in chapter 4 and an assessment of the performance of the potential wind gust techniques will be presented.

3.4 Adaptation of the AWS ET/VIL Table

Since no equation exists for the AWS ET/VIL table, a method to evaluate this technique for values that do not appear on the table needed to be developed. It was assumed that the equation which would fit the surface of this table would be of the same form as Stewart's equation. The values of the AWS table were then regressed using Microsoft Excel©. The following is the equation that resulted:

$$w = \left[(15.780608VIL) - (2.3810964 \times 10^{-6} ET^2\right]^{1/2} \quad (8)$$

The R squared value for this regression was 0.988 indicating the model fit the surface very well. The difference between the model and the AWS table is shown in Table 5.

ET (kft) \ VIL (kg m^{-2})	15	20	25	30	35	40	45	50	55	60	65	70
60								**10**	0	-1	0	0
55							0	0	0	0	-1	0
50					**9**	-1	0	0	0	0	0	-1
45				0	0	0	0	0	0	0	-1	-1
40		**9**	3	0	0	0	-1	0	-1	0	0	0
35	**13**	5	1	-1	-1	-1	0	-1	0	0	0	0
30	6	2	1	0	0	0	-1	0	-1	0	0	0
25	4	2	1	0	2	1	1	0	0	0	-1	-1
20	2	2	2	2	2	3	2	1	1	-1	0	-2
15	2	2	2	3	4	3	3	2	1	0	0	-2

Table 5. Difference (kts) between AWS table and model

The bold numbers indicate values present on the AWS table that were not calculated using the regression model. Based on the above results, this regression model will be used to evaluate the AWS ET/VIL table.

4. Data Analysis and Discussion

4.1 Introduction

The steps outlined in chapter 3 were completed on 58 potential microburst days leaving 11 candidate days. After the final 11 candidate days were examined, 15 microburst events were identified. It must be noted that with such a small sample size, the results of this analysis cannot be taken as conclusive. This chapter analyzes the data collected and provides preliminary insight into the performance of the three techniques used to predict downburst winds from thunderstorms. Both subjective and objective tools were used to accomplish this. Scatterplots were used to subjectively compare the observed gusts with the predicted gusts. The objective tools were the root mean squared error (RMSE) and mean absolute error (MAE) of the predicted gust when compared to the observations. The standard deviation of the AE was also calculated to provide a measure of the variance of the error. An operational assessment was also conducted.

4.2 Assumptions Used During Analysis

There were several assumptions used during the analysis of the data collected. Knowing these assumptions and understanding their implications is vital to understanding the sources of error that may have affected the results. The following summarizes these assumptions and implications.

1) Wind gust magnitude recorded by WINDS network is the true magnitude of the downburst. Recording the actual speed of the wind upon impact with the ground would be virtually impossible. The thunderstorm would have to collapse almost instantaneously directly above a wind sensor for this to be accomplished. It is important

to note that since the cell was located at a distance from the sensor that the actual magnitude may have been decreased by friction or actually have increased due to acceleration of the ring vortex or the meso-high created by the downburst itself (Stewart, 1991:16; Roeder, 1998).

2) The direction of the wind recorded by the WINDS network is the direction of the gust. The WINDS network records wind data at five minute intervals. The direction recorded is the five-minute average direction recorded in the subsequent five-minute period after the time indicated. The direction of the gust is needed to calculate the amount of environmental wind correction to add when using the vector correction factor. If the direction recorded and the true direction of the gust differ significantly, the correction factor will be erroneous.

3) The time of the gust reported by the WINDS network is the actual time of the gust. As previously mentioned, the WINDS network reports values in five-minute increments. It reports the gust wind speed recorded in the subsequent five-minute period. Therefore, the gust could have occurred up to, but not including, five minutes later than recorded.

4) The Velocity Azimuth Display (VAD) Wind Profile (VWP) represents the true wind profile of the atmosphere at the time. The mean surface-5,000 feet wind speed and direction are required to calculate the environmental wind correction factor. The most readily available source of such information for the forecaster is the VWP. If the VWP does not truly represent the actual atmosphere, then error in the correction factor, and subsequently the gust forecast, will occur.

5) The values reported by the WATADS algorithms are correct and exact. This includes the time of the volume scan being the exact time the radar signature occurred. Also, the location of the storm centroid is assumed correct and instantaneous. It is possible that the storm will move during the processing of the volume scan but accounting for that motion is not possible. Finally, because of the timescale in which microbursts occur, it is feasible that an event may happen between volume scans.

4.3 Analysis Tools

4.3.1 Scatterplots

Scatterplots were created to visually display the accuracy of the forecast technique. Plotting the observed gust value on the ordinate and the predicted gust value on the abscissa gives insight on how close the forecast was to the corresponding observation. In such a configuration, perfect forecasts would result in the plots falling on a 45-degree line. Underestimated forecasts are plotted above the line whereas over-forecasts are plotted under the line. The scatterplots for all forecasting techniques studied in this thesis can be found in Appendix B.

4.3.2 Correlation

To get a measure of the association between the forecasts and observations, the Pearson correlation coefficient, r, was calculated. The correlation coefficient, as it is commonly referred to, is used to assess if a linear relationship between two variables exists. The value of r is bound by –1 and 1. The extremes represent perfect negative or positive correlation respectively (Wilks 1995:45). The value approaches zero as the likelihood of a linear relationship between the two variables diminishes. For this study, a

correlation approaching 1 would indicate that the forecasts were close to the observations.

4.3.3 Root Mean Squared Error

A scalar value used to measure the accuracy of a forecast technique is the root mean squared error (RMSE). The RMSE is defined as

$$RMSE = \left[\frac{1}{n} \sum_{k=1}^{n} (observed_k - predicted_k)^2 \right]^{1/2} \quad (9)$$

The RMSE can represent the typical magnitude of the forecast error (Wilks, 1995:254).

4.3.4 Mean Absolute Error

Another value used to represent forecast error is the mean absolute error (MAE). The MAE is defined as

$$MAE = \frac{1}{n} \sum_{k=1}^{n} \left| observed_k - predicted_k \right| \quad (10)$$

The MAE also represents the typical magnitude of forecast error but is not as sensitive to large errors as RMSE since there is no squared term.

4.4 Analysis of Stewart's ET/VIL WGP Technique

The original ET/VIL WGP technique developed by Stewart in 1991 required the vector addition of 1/3 the mean surface-5,000 feet winds, subsequently referred to as the environmental wind . This correction factor was used to account for the mixing of horizontal momentum in the lower levels (Stewart, 1991:7). Frazier (1994) evaluated the technique using data from the northeastern United States. He found that addition of 100% of the environmental winds provided higher correlation of the observed gusts to the

predicted gusts. In order to provide a comparison of various correction factors, seven different schemes were used. The final potential wind gust was calculated by first calculating the WGP using equation 6. Then a portion of the mean environmental was added. The portions and addition method were: no correction, 1/3 vectorally, 1/2 vectorally, 100% vectorally, 1/3 algebraically, 1/2 algebraically, 100% algebraically.

Table 6 summarizes the predictions using Stewart's technique with the various correction schemes.

Julian Date	Observed	No Corr	1/3 Vec Corr	1/2 Vec Corr	100% Vec Corr	1/3 Alg Corr	1/2 Alg Corr	100% Alg Corr
94174	55	35	33	32	29	41	44	52
94176	46	43	42	42	42	48	50	58
94201#1	36	43	38	36	28	51	54	66
94201#2	35	41	43	43	45	46	48	55
94210	40	47	52	54	62	52	55	63
96226	35	53	53	54	55	56	58	63
97170	59	49	48	48	47	53	54	60
97210#1	44	32	35	36	41	35	36	41
97210#1	53	31	33	34	37	34	36	41
97232#1	44	24	27	28	31	28	30	35
97232#2	46	47	50	52	58	51	52	58
98199	35	44	46	47	50	46	47	50
98209#1	52	47	49	50	52	49	51	55
98209#2	52	49	50	51	53	51	52	55
98226	54	56	56	56	56	57	58	61

Table 6. Stewart's ET/VIL WGP (kts) Summary The various correction schemes are abbreviated as follows: Vec Corr = vectoral correction and Alg Corr = algebraic correction.

The numeric statistics for Stewart's ET/VIL technique with the various correction factors are summarized in Table 7.

	No Corr	1/3 Vec Corr	1/2 Vec Corr	100% Vec Corr	1/3 Alg Corr	1/2 Alg Corr	100% Alg Corr
Correlation	-0.01	-0.01	-0.01	-0.04	-0.04	-0.06	0.05
P-value	0.97	0.97	0.96	0.88	0.89	0.83	0.64
RMSE (kts)	11.9	11.8	12.0	13.4	11.6	12.0	15.1
MAE (kts)	9.7	9.7	9.7	10.9	9.9	10.1	12.1
SD of AE	7.1	7.0	7.4	8.0	6.4	6.7	9.5
Hits	5	6	5	5	5	5	5

Table 7. Stewart's ET/VIL Statistics Summary

4.5 Analysis of AWS ET/VIL WGP

The performance of the ET/VIL WGP table that appeared in ECHOES #16 is of great interest to the 45 WS. This is the table they use operationally to help determine the potential wind gusts of a thunderstorm. The regression equation detailed in chapter 3 was used to calculate WGP and the correction factor schemes outlined above were added to determine the final gust potential. Table 8 summarizes the final gust predictions.

Julian Date	Observed	No Corr	1/3 Vec Corr	1/2 Vec Corr	100% Vec Corr	1/3 Alg Corr	1/2 Alg Corr	100% Alg Corr
94174	55	31	29	28	25	36	39	48
94176	46	38	37	37	36	43	45	53
94201#1	36	38	33	30	23	45	49	61
94201#2	35	36	38	38	40	41	43	50
94210	40	41	46	48	56	46	49	57
96226	35	46	47	47	48	49	51	56
97170	59	43	42	42	41	47	48	54
97210#1	44	28	31	32	37	31	32	37
97210#1	53	27	29	30	34	30	32	37
97232#1	44	21	24	25	29	25	27	32
97232#2	46	41	45	46	52	45	47	52
98199	35	39	41	42	45	41	42	45
98209#1	52	41	43	44	47	44	45	49
98209#2	52	43	44	45	47	45	46	49
98226	54	49	49	49	50	50	51	54

Table 8. AWS ET/VIL WGP (kts) Summary

The numeric statistics for the AWS ET/VIL technique with the various correction factors are summarized in Table 9.

	No Corr	1/3 Vec Corr	1/2 Vec Corr	100% Vec Corr	1/3 Alg Corr	1/2 Alg Corr	100% Alg Corr
Correlation	0.02	-0.03	-0.01	-0.03	-0.04	-0.09	-0.15
P-value	0.94	0.92	0.97	0.91	0.88	0.76	0.59
RMSE (kts)	13.5	13.2	13.1	13.6	11.8	11.5	12.4
MAE (kts)	10.8	10.8	10.9	11.7	10.0	10.0	10.3
SD of AE	8.0	8.0	8.0	7.0	6.5	6.0	7.2
Hits	6	4	3	4	3	3	4

Table 9. AWS ET/VIL Statistics Summary

4.6 Analysis of the d/H WGP Technique

Similarly, the d/H WGP technique data are summarized in Table 10. As with the previous techniques, the d/H WGP technique had inconsistent success. Also, review of the data shows that this technique may be high biased. This bias will be addressed in section 4.8.

Julian Date	Observed	Predicted
94174	55	111
94176	46	52
94201#1	36	86
94201#2	35	50
94210	40	67
96226	35	93
97170	59	73
97210#1	44	58
97210#1	53	55
97232#1	44	49
97232#2	46	48
98199	35	84
98209#1	52	63
98209#2	52	82
98226	54	67

Table 10. d/H WGP (kts) Summary

Table 11 details the statistics for the d/H technique.

Correlation	P-value	RMSE (kts)	MAE (kts)	SD of AE	Hits
0.02	0.94	30.6	23.5	20.3	3

Table 11. d/H WGP Statistics Summary

4.7 Analysis of the ST/VIL WGP Technique

Wind Gust Potentials were calculated using the Storm Top and VIL. These predictions are summarized in Table 12. Again, the ST/VIL technique had inconsistent success at forecasting the wind gust. Possible reasons for this inconsistency is discussed in Section 4.11.

Julian Date	Observed	Predicted
94174	55	52
94176	46	42
94201#1	36	51
94201#2	35	37
94210	40	50
96226	35	56
97170	59	51
97210#1	44	40
97210#1	53	39
97232#1	44	31
97232#2	46	48
98199	35	49
98209#1	52	46
98209#2	52	48
98226	54	55

Table 12. ST/VIL WGP (kts) Summary

The statistics for the ST/VIL technique are shown in Table 13.

Correlation	P-value	RMSE (kts)	MAE (kts)	SD of AE	Hits
0.10	0.73	10.0	8.1	6.1	7

Table 13. ST/VIL Statistics Summary

4.8 Bias

If a forecast technique consistently predicts a gust that is higher than observed then the technique may be high biased. Likewise, if the prediction is consistently lower

than observed, the technique may be low biased. The scatterplots can used to see if bias is affecting the performance of a forecast technique. If a significant number of points lay on the same side of the 45-degree line then this might suggest bias exists.

The scatterplots in Appendix B show that there may exist a high bias for the d/H WGP technique since most of the points lay below the 45-degree line. The data for the d/H WGP technique were then analyzed to quantify the bias. The mean observed and predicted gusts were calculated, and the difference between the means was 23 knots. The predicted gusts were then adjusted by subtracting 23 knots from each value. The numerical statistics were then recalculated. The statistical results are shown in Table 14.

Correlation	P-value	RMSE (kts)	MAE (kts)	SD of AE
0.02	0.94	19.6	17.1	9.8

Table 14. d/H WGP Technique with Bias Adjustment Summary

This shows that some improvement was achieved by adjusting the forecasts based on the calculated bias, for this data set. Since the data set is so small, applying this bias to future predictions is not prudent. This does suggest, however, that with a larger data set, a systematic bias could be realized and applied generally to future forecasts using the d/H WGP technique, at a given location. The scatterplots for the other techniques, shown in Appendix B, did not show that bias was evident.

4.9 Operational Assessment

The numeral analysis presented above gives values for the average error found for the various techniques. However, these statistics, i.e., the RMSE and MAE, can be misleadingly impacted by a relatively small number of forecasts that are significantly different than the corresponding observations. For example, in a sample size of 10

observations, if 9 forecasts were exact but one forecast was off by 15 knots, the RMSE calculated would be 5 knots. This error doesn't represent the majority of the forecasts. To provide further insight into performance of the WGP techniques studied for this thesis, two additional means of analysis were used.

First, the techniques were assessed by assuming that a forecast that was within 5 knots of the observed gust was a "good" forecast and constituted at "hit." Tables 15-17 summarize how many hits each technique had.

	No Corr	1/3 Vec Corr	1/2 Vec Corr	100% Vec Corr	1/3 Alg Corr	1/2 Alg Corr	100% Alg Corr
Hits	5	6	5	5	5	5	5

Table 15. Stewart's ET/VIL Hits

	No Corr	1/3 Vec Corr	1/2 Vec Corr	100% Vec Corr	1/3 Alg Corr	1/2 Alg Corr	100% Alg Corr
Hits	6	4	3	4	3	3	4

Table 16. AWS ET/VIL Hits

	d/H	ST/VIL
Hits	3	7

Table 17. d/H and ST/VIL Hits

The second method assesses how many forecasts were hits for the corresponding warning categories. In other words, how many forecasts within the 35 to <50 knots range were correct. Likewise, how many of the ≥ 50 knot forecasts were correct. Since the greater than 60 knot category is unique to KSC, it was not assessed. Also, since there was no significant improvement using an environmental wind correction factor for the

ET/VIL techniques, only the base predictions were assessed in this section. Tables 18-21 summarize this assessment.

	< 35 knots	35 - < 50 knots	≥ 50 knots
Observations	0	9	6
Forecasts	3	10	2
Correct	0	8	1

Table 18. Stewart's ET/VIL Forecast Hits

	< 35 knots	35 - < 50 knots	≥ 50 knots
Observations	0	9	6
Forecasts	4	11	0
Correct	0	7	0

Table 19. AWS ET/VIL Forecast Hits

	< 35 knots	35 - < 50 knots	≥ 50 knots
Observations	0	9	6
Forecasts	0	2	13
Correct	0	2	6

Table 20. d/H Forecast Hits

	< 35 knots	35 - < 50 knots	≥ 50 knots
Observations	0	9	6
Forecasts	1	8	6
Correct	0	5	5

Table 21. ST/VIL Forecast Hits

These tables show that it may be feasible to pursue using these techniques as a categorical forecast tool as opposed to trying to forecast the exact magnitude of wind gust. This, of course, would require the acquisition of a much larger data set to make the analyses more statistically significant.

4.10 Lead-time and Distance Analysis

During the data acquisition phase of this research, the volume scan time and the time of event were recorded. Using the recorded times, the lead-time of an event can be calculated. The same volume scan, the one that reported maximum VIL value prior to the event, was used for the techniques that used VIL. The d/H technique used the volume scan with the highest maximum reflectivity value. The mean lead-times and standard deviations are summarized below.

	VIL Techniques	d/H Technique
Max	38	36
Min	9	2
Mean	18	20
S. D.	8	8

Table 22. Lead-time (min) Summary

Caution must be used when interpreting these lead-times. Since the radar uses 5-6 minutes, depending on VCP, to complete a volume scan, the exact time the signature occurred is not known. Also, the WINDS network reports data for the five-minute period after the time of record. Therefore, it is possible that there be as much as an 11 minute error in the lead-times recorded. Finally, since these techniques are designed to predict the potential wind gust of a thunderstorm, not the probability of thunderstorm creating a downburst, one should not use this information in an attempt to meet the 45 WS lead-time requirements. This information is only included for completeness.

The azimuth and range of the storm centroid were also recorded during the data acquisition phase of this thesis. With this information, using the Mathcad© templates in Appendix D, the approximate distance between the storm centroid and the recording tower was calculated. Knowledge of this distance is important since it is possible the

gust magnitude may have decreased due to frictional drag or even increased due to acceleration of the vortex ring or the meso-high. The closer a storm is to a tower, the more probable that the recorded gust magnitude is the magnitude of the downburst upon impact with the ground. The distance information is summarized in Table 23.

	VIL Techniques	d/H Technique
Max	10.1	10.9
Min	1.9	2.0
Mean	5.0	6.3
S. D.	2.4	2.8

Table 23. Average Distance (nm) between Centroids and Sensors

During his research, Stewart used only storms that were within 5 nautical miles of the recording device (Stewart, 1998). To determine if a relationship between distance and gust speed could be determined using the data from this thesis, the events that were greater than 5 nautical miles away from the recording tower were removed from the calculations. This reduction left 10 events for the VIL techniques and 6 for the d/H technique. Table 24 compares both sets of data.

		RMSE (kts)	MAE (kts)	SD of AE (kts)
Stewart's ET/VIL (No Corr)	Complete set	11.9	9.7	7.1
	Reduced set	12.5	10.0	7.9
AWS ET/VIL (No Corr)	Complete set	13.5	10.8	8.0
	Reduced set	14.3	12.3	7.7
d/H	Complete set	30.6	23.5	20.3
	Reduced set	32.0	23.5	23.9
ST/VIL	Complete set	10.0	8.0	6.0
	Reduced set	10.6	8.5	6.6

Table 24. Reduced Data Set Comparison

This analysis shows that the effect of distance of the storm from the tower on the wind gust speed cannot be determined. If events with distances greater than 5 nautical miles had been negatively affecting the analysis of the complete set then the statistics of the reduced set should have improved. However, the statistics actually got worse, for the most part. Therefore, attempting to quantitatively determine the effect of distance is not practical.

4.11 Possible Sources of Error

It is clear, even with this small sample size, that the performance of the three prediction techniques, along with the different correction schemes, varies greatly. These results showed that in one situation, a technique predicted the exact magnitude of the observed wind. In another, an absolute error of 36 knots was observed. There are several factors that may explain why these results aren't comparable to the 0.95 correlation Stewart found for the ET/VIL WGP technique (Stewart, 1996:325).

One reason that might explain why such large errors were found for this thesis is that Stewart (and Frazier) used a different radar system to perform their studies. They used the WSR-57 RADAP II system. This older system has a resolution for the VIL and ET products, (3 by 5 nm.) By contrast, the WSR-88D uses a resolution of 2.2 nm by 2.2 nm. This results in values being assigned to different grid boxes that may have been assigned to the same grid box using the WSR-57. Since a storm may occupy more than one grid box, the complete parameter value for that storm may not be estimated correctly.

Examples where this might be the case are the two different storms on 29 Jul 97. On this day, the first observed gust was 44 knots. The ET and VIL values from the storm were 43 and 39 respectively giving a predicted wind gust of only 32 knots. Assuming that the ET value is correct, the VIL would have to be 51 to have a prediction of 44 knots. Similarly, the second storm produced an observed gust of 53 knots. The ET and VIL were 42 and 37 respectively predicting a gust of 31. Had the VIL value been 61, a gust of 53 would have been predicted. It is feasible that these storms occupied two adjacent VIL grid-boxes and, thus, the VIL algorithm reported lower values than it would have if the storms were completely in one grid-box. The ET value should not be significantly different, however, since the algorithm simply reports the height of the highest 18 dBZ reflectivity for the grid. Two other storms investigated showed similar possibilities.

Another source of error is the fact that the prediction equation (4) assumes a standard tropical atmosphere to calculate the coefficients (Stewart, 1998). If the true atmosphere deviates from this standard atmosphere, the prediction equation will not perform correctly. The equation (4) was tuned using a mean mid-level θ_e of 328.5 K. If the true mean θ_e is lower, the equation (4) will underestimate the wind gust. Likewise, a higher mean θ_e will result in an overestimation.

The storm on 14 Aug 95 may illustrate the effect of a thermodynamic profile that deviated from the standard. The mean mid-level θ_e for that day was 334K, a difference of over 5K from the assumed value. Using Stewart's ET/VIL WGP technique, a gust of 53 knots was predicted. The actual gust observed was only 35 knots. The lower observed gusts may be a result of the atmospheric conditions not providing the evaporative cooling necessary to create a downburst of the magnitude expected. This

possibility existed in six other cases studied. In the remaining eight, however, the opposite was true. The mean θ_e was greater than 328.5K, yet the observed gust was greater than predicted. With this small sample size, it cannot be conclusively determined exactly how the actual mean θ_e will affect the gust. This analysis does show a possibility that the relationship described above exists. There could be other unknown factors involved that affected the eight cases that didn't follow this relationship.

Other possible sources of error are the limitations of VIL and ET algorithms outlined in chapter 3. Because of these limitations the true storm parameters may not be correctly represented thus causing the WGP techniques to under or over forecast. Also, the modification to the WATADS SCIT algorithm that simulated the ET algorithm may not have correctly calculated the ET . Therefore, the forecasted gust would also be incorrect. Finally, due to the timescale in which microburst events take place, the radar may not have the ability to resolve the features necessary to accurately predict the wind gusts associated with microbursts.

5. Summary and Conclusion

5.1 Restatement of Problem

The 45 WS required the evaluation of three radar-based techniques used to predict downdraft wind gusts. These techniques are, the Echo Top/ Vertically Integrated Liquid Wind Gust Potential (ET/VIL WGP), Maximum Reflectivity/ Height of Maximum Reflectivity (d/H) Wind Gust Potential, and the Storm Top/Vertically Integrated Liquid (ST/VIL) Wind Gust Potential techniques.

5.2 Summary of Methodology and Results

This research focused on pulse-type thunderstorms in an atmosphere conducive for downbursts to occur. The methodology entailed eliminating storms that occurred on days where significant synoptic features, e.g., fronts and hurricanes, were affecting the CCAS/KCS locale. The NOAA *Daily Weather Maps* were used to accomplish this step. The thermodynamic profile for the remaining days was then analyzed to determine if dry, cold air was present in the mid-levels to allow for the evaporative cooling required to produce a downburst. This screening process left 15 storms that met the requirements for inclusion in the study. The radar data were then analyzed and the required parameters for the 15 storms recorded. Using these parameters, wind gust forecasts were calculated and compared to the observed gusts. A statistical analysis was completed to give an assessment of the performance of the four wind gust potential techniques. These statistics are summarized in the following Table 25.

	Stewart's ET/VIL	AWS ET/VIL	d/H	ST/VIL
RMSE (kts)	11.9	13.5	30.6	10.0
MAE (kts)	9.7	10.5	23.5	8.1
S.D. of AE (kts)	7.1	8.0	20.3	6.1
HITS (out of 15)	5	6	3	7

Table 25. Summary of Statistics

5.3 Operational Consideration

Due to the method in which the WSR-88D reports ET and VIL to the user, an intrinsic error is present. The ET and VIL products display values in 5 kft and 5 Kg m^{-2} lower-bounded bins, respectively. The forecaster is unable to determine the exact value that was calculated by the algorithms. Because of this, the WGP may vary greatly. For example, if the WSR-88D products display a storm with an ET of 40 kft and a VIL of 35 Kg m^{-2} then the WGP using Stewart's table (Table 2) is 31 knots. However, if the true values for the storms ET and VIL were 40 kft and 39 Kg m^{-2}, the displays would be the same but calculated WGP is 36 knots. Similarly, if the true values for the storms ET and VIL were 44 kft and 35 Kg m^{-2} the calculated WGP is 25 knots. A difference of 11 knots exists with the same displayed ET and VIL values. Table 26 shows the possible error for each operational combination of ET and VIL. This can be interpreted as a finite-difference estimate of the maximum slope of the surface at the given point in the domain.

ET (kft) \ VIL (kg m^{-2})	15	20	25	30	35	40	45	50	55	60	65	70
60										19	14	12
55								21	14	12	10	9
50							15	12	10	9	8	7
45					19	13	10	9	8	7	7	6
40				15	11	9	8	7	7	6	6	6
35			14	10	9	8	7	6	6	6	5	5
30		13	10	8	7	6	6	5	5	5	5	4
25	12	9	8	7	6	6	5	5	5	4	4	4
20	9	7	6	6	5	5	5	4	4	4	4	4
15	7	6	5	5	5	4	4	4	4	3	3	3

Table 26. ET/VIL Operational Error (kts)

5.4 Conclusions

The performances of the four WGP techniques studied for this thesis were extremely variable. In some cases, the techniques were very close in predicting the magnitude of the gust, while in others, there were considerable differences. Additionally, no systematic explanations were apparent in determining why the techniques produced an accurate forecast for some storms and not others. Table 25 summarizes the average errors for each technique and the number of times the technique was within 5 knots of the observed gusts.

Although no one technique performed significantly better than the others, the ST/VIL WGP technique had the lowest RMSE, MAE, standard deviation of AE, and the highest number of forecasts within 5 knots. Also, the d/H WGP technique had the highest RMSE, MAE, standard deviation of AE, and the lowest number of forecasts within 5 knots. Because of the small sample size, however, these results cannot be considered conclusive but may indicate that use of these techniques operationally may not give the degree of accuracy required by the 45 WS.

Finally, if the use of the ET/VIL WGP technique is continued, Stewart's table should replace the AWS ET/VIL table. No scientific reason was found to explain the deviation of the AWS ET/VIL WGP table from Stewart's. Use of the AWS ET/VIL WGP table is not scientifically justified.

5.5 Recommendations for Further Study

There are three recommendations for future research. First, increase the sample size in order to make the analyses more statistically significant. Second, study the relationship between the value of the mid-level θ_e and the WGP equation (4) and stratify the ST/VIL table accordingly. Finally, focus more attention on the Damaging Downburst Prediction and Detection Algorithm (DDPDA)[1] being developed by the WSR-88D Operational Support Facility.

[1] http://www.nssl.noaa.gov/~tsmith/ddpda/index.html

Appendix A: Acronyms

AFCCC	Air Force Combat Climatology Center
AFWA	Air Force Weather Agency
AMU	Applied Meteorology Unit
AWS	Air Weather Service
CCAS/KSC	Cape Canaveral Air Station/Kennedy Space Center
CT	Cell Trends
d/H	Maximum Reflectivity/Height of Maximum Reflectivity
DDPDA	Damaging Downburst Prediction and Detection Algorithm
ET	Echo Top
FMH-11	Federal Meteorological Handbook 11
FWGP	Final Wind Gust Prediction
JAWS	Joint Airport Weather Study
MAE	Mean Absolute Error
MIST	MIcroburst and Severe Thunderstorm Study
NCDC	National Climatic Data Center
NEXRAD	NEXt GENeration radar
NIMROD	Northern Illinois Meteorological Research On Downbursts
NOAA	National Oceanic and Atmospheric Association
NSSL	National Severe Storms Laboratory
NWS	National Weather Service
PAM	Portable Automated Mesonet
PUP	Principle User Processor
RDA	Radar Data Acquisition unit
RMSE	Root-Mean Squared Error
SCIT	Storm Cell Identification and Tracking algorithm
SLF	Shuttle Landing Facility
ST	Storm Top
UTC	Universal Time Coordinated
VAD	Velocity Azimuth Display
VCP	Volume Coverage Pattern
VIL	Vertically Integrated Liquid
VWP	VAD Wind Profile
WATADS	WSR-88D Algorithm Testing And Display System
WGP	Wind Gust Potential
WINDS	Weather Information Network Display System
WSR-88D	Weather Surveillance Radar 88 Doppler

Appendix B: Scatterplots

This appendix contains the 16 scatterplots produced using the data for the four Wind Gust Potential prediction techniques evaluated in this thesis. The observed gust is plotted on the vertical axis and the predicted gust is plotted on the horizontal axis. A perfect forecast will fall on a 45-degree line. The relative distance from the 45-degree line is indicates the relative error in the forecast.

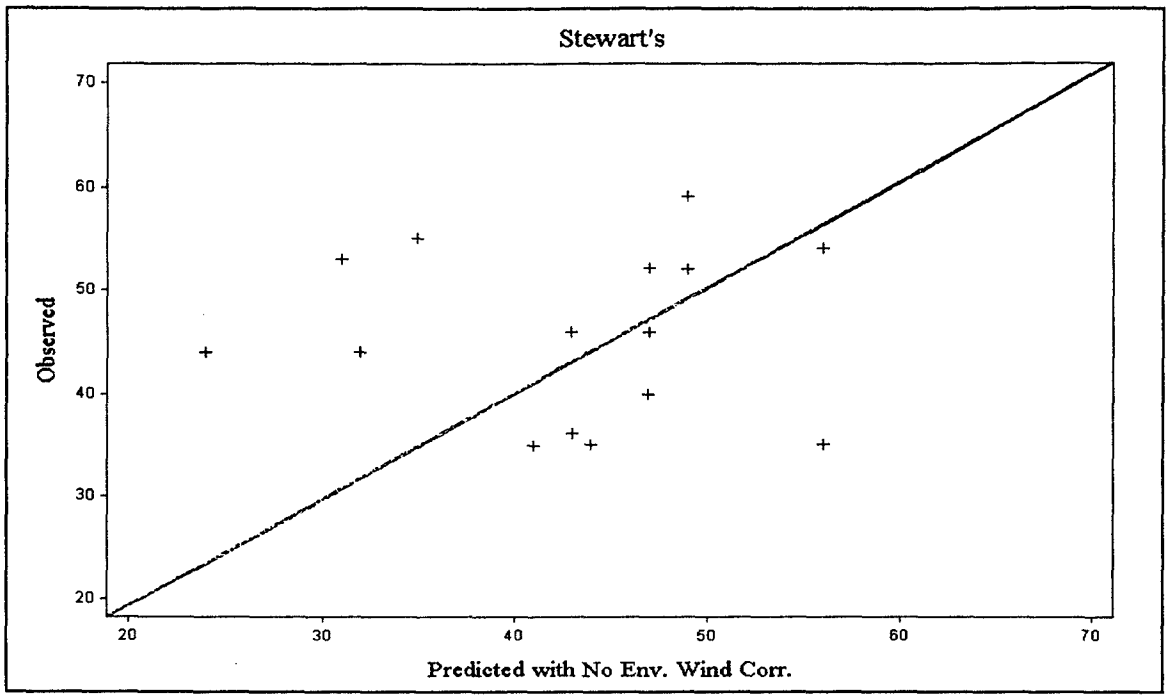

Figure 12. Stewart's ET/VIL WGP with No Env. Wind Correction

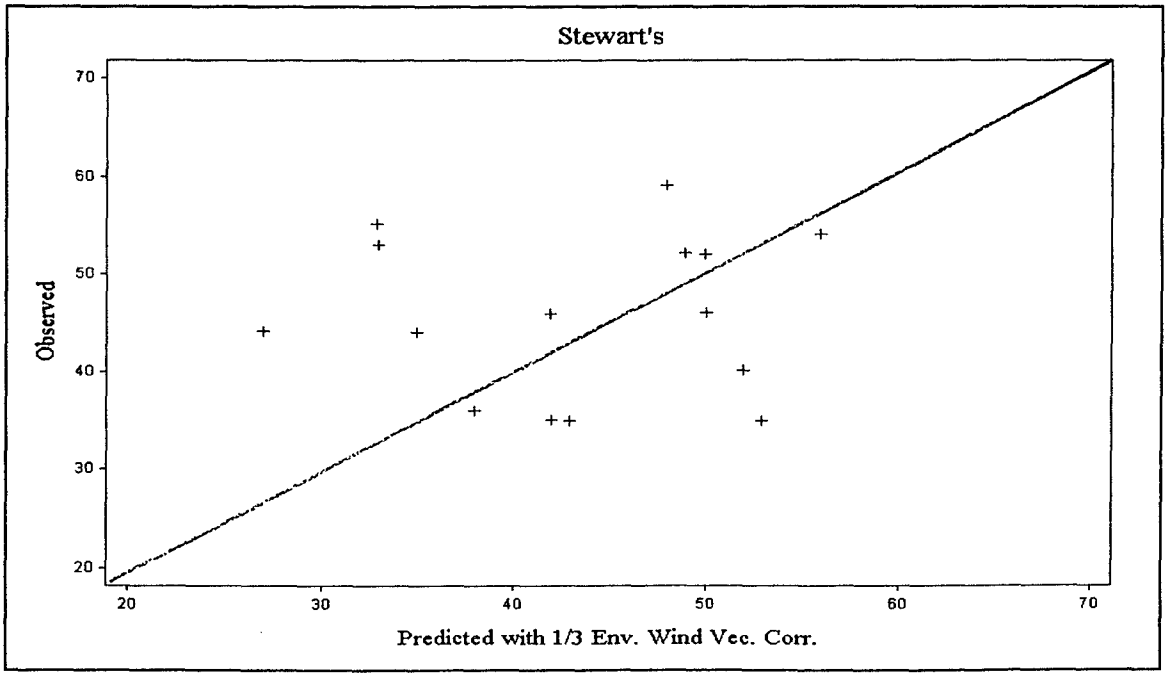

Figure 13. Stewart's ET/VIL WGP with 1/3 Env. Wind Vector Correction

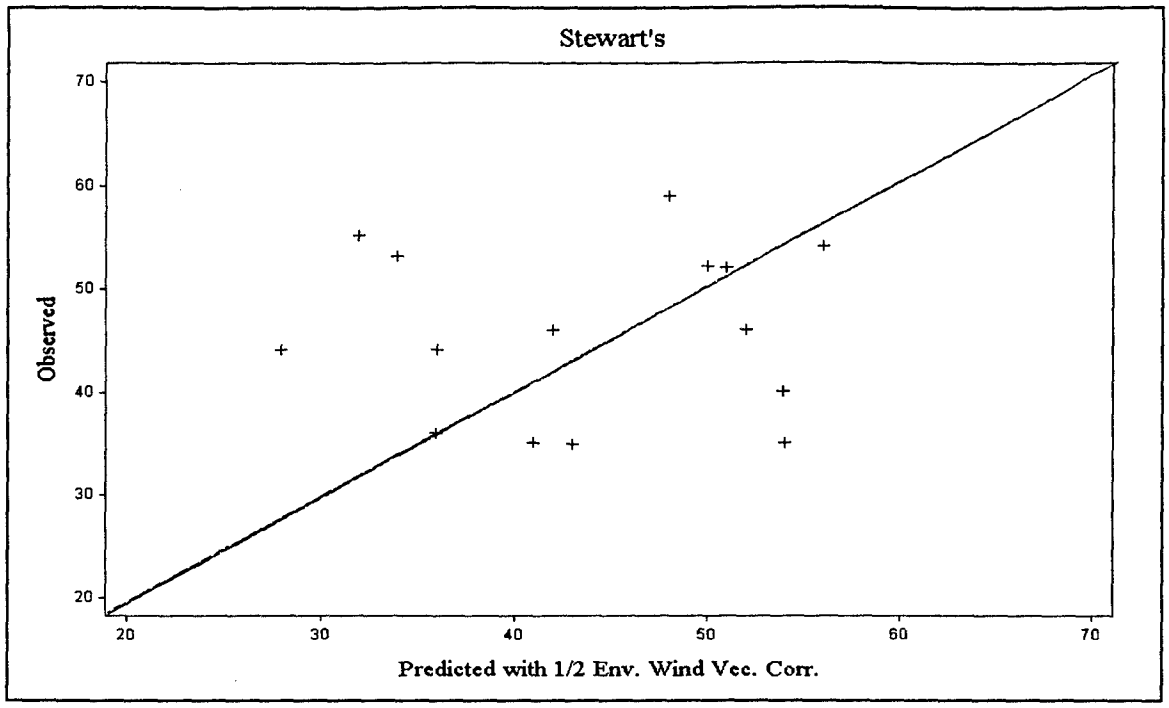

Figure 14. Stewart's ET/VIL WGP with 1/2 Env. Wind Vector Correction

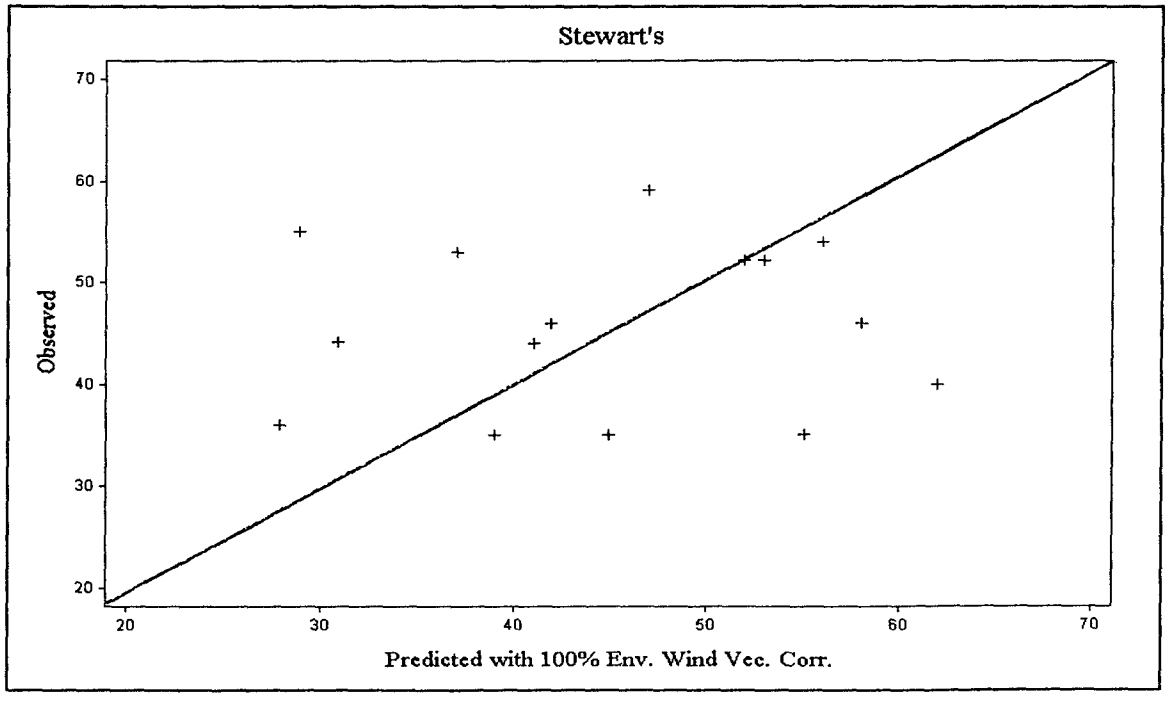

Figure 15. Stewart's ET/VIL WGP with 100% Env. Wind Vector Correction

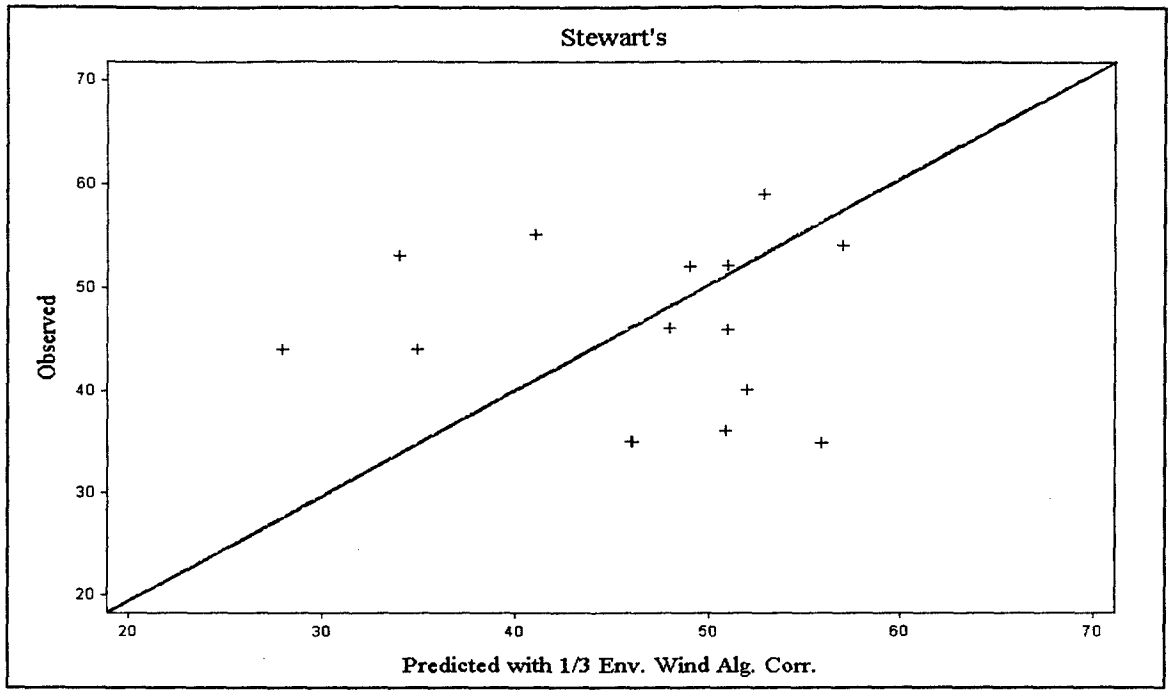

Figure 16. Stewart's ET/VIL WGP with 1/3 Env. Wind Algebraic Correction

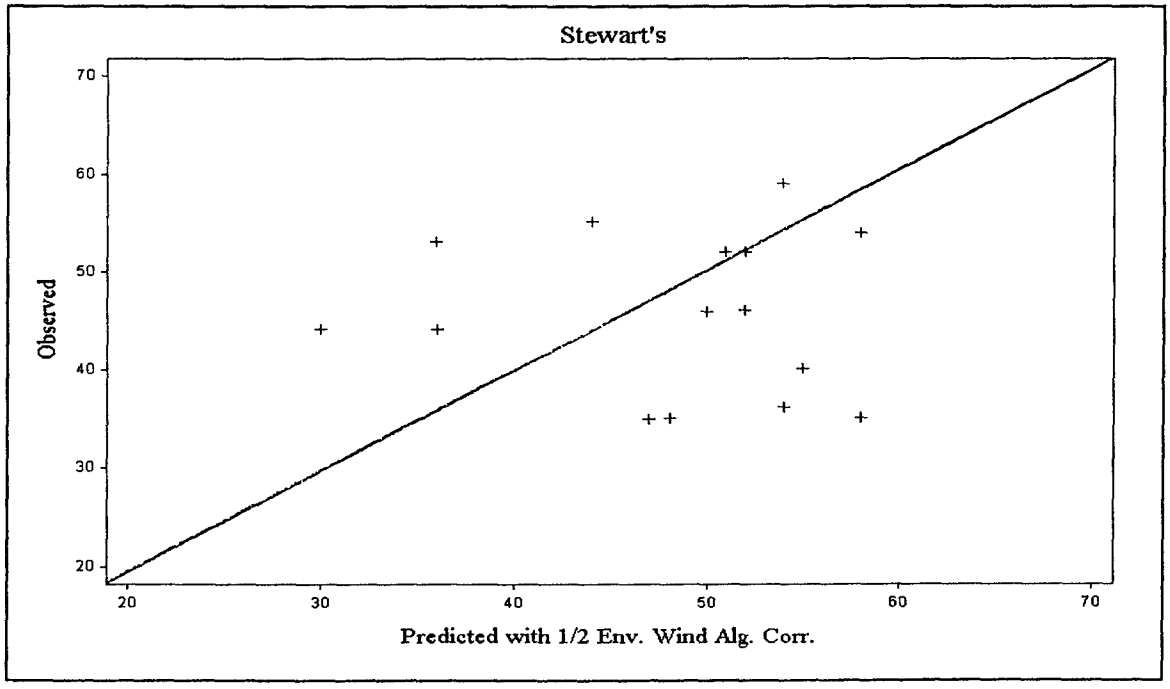

Figure 17. Stewart's ET/VIL WGP with 1/2 Env. Wind Algebraic Correction

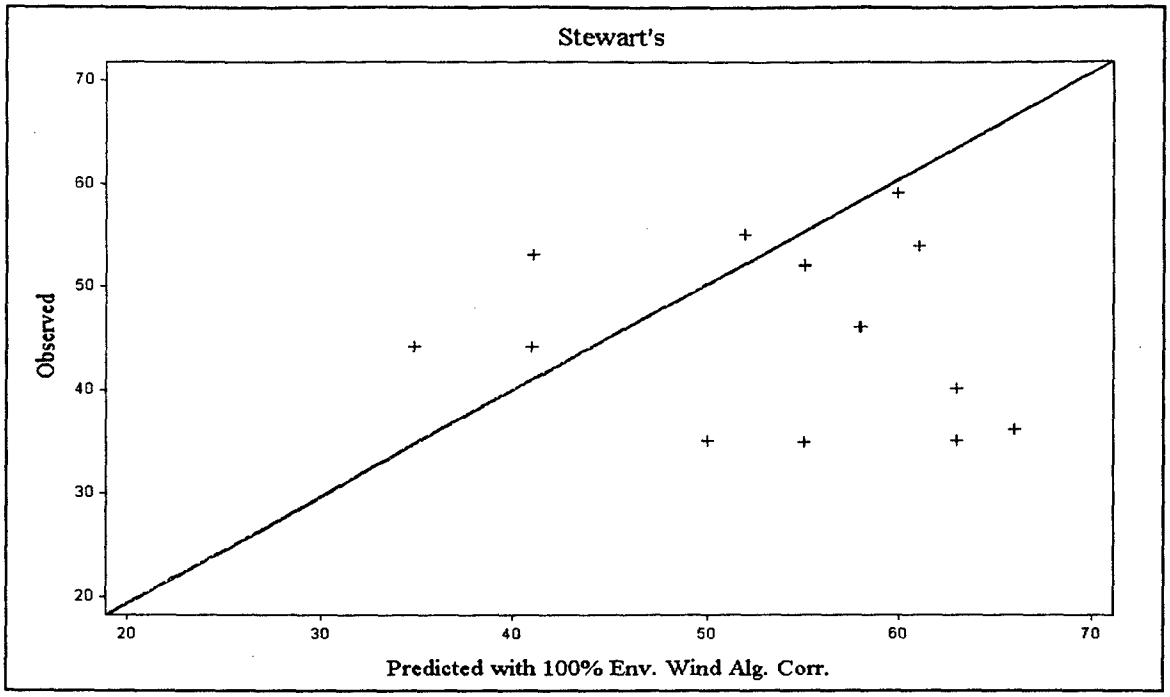

Figure 18. Stewart's ET/VIL WGP with 100% Env. Wind Algebraic Correction

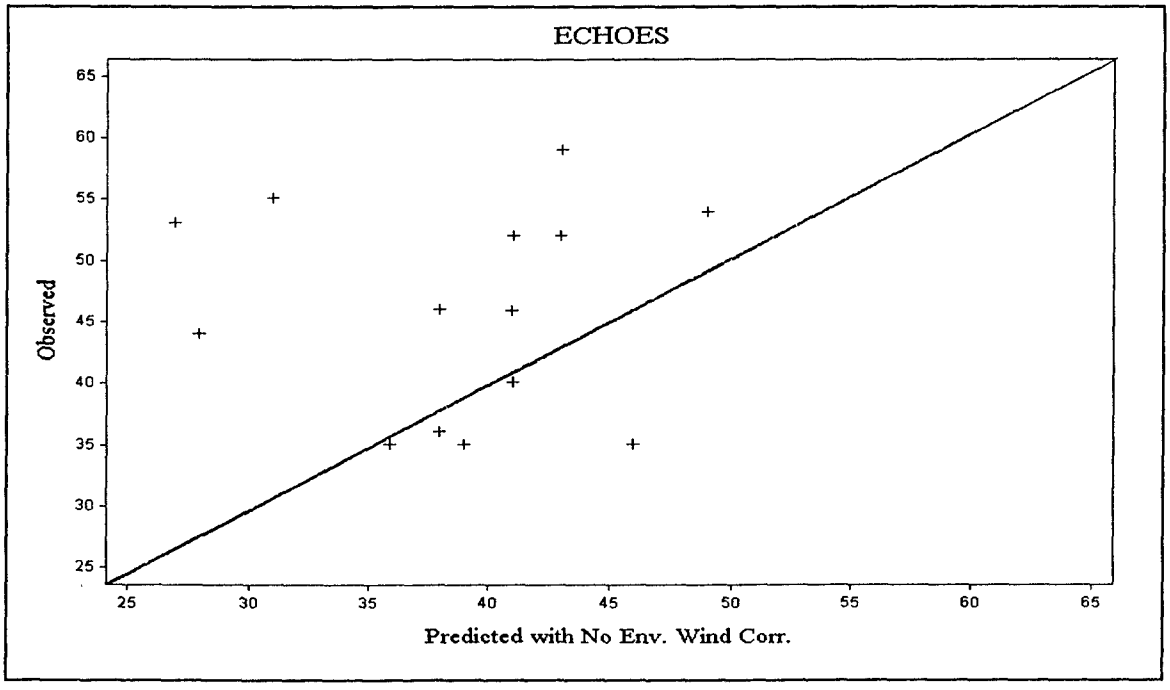

Figure 19. AWS ET/VIL WGP with No Env. Wind Correction

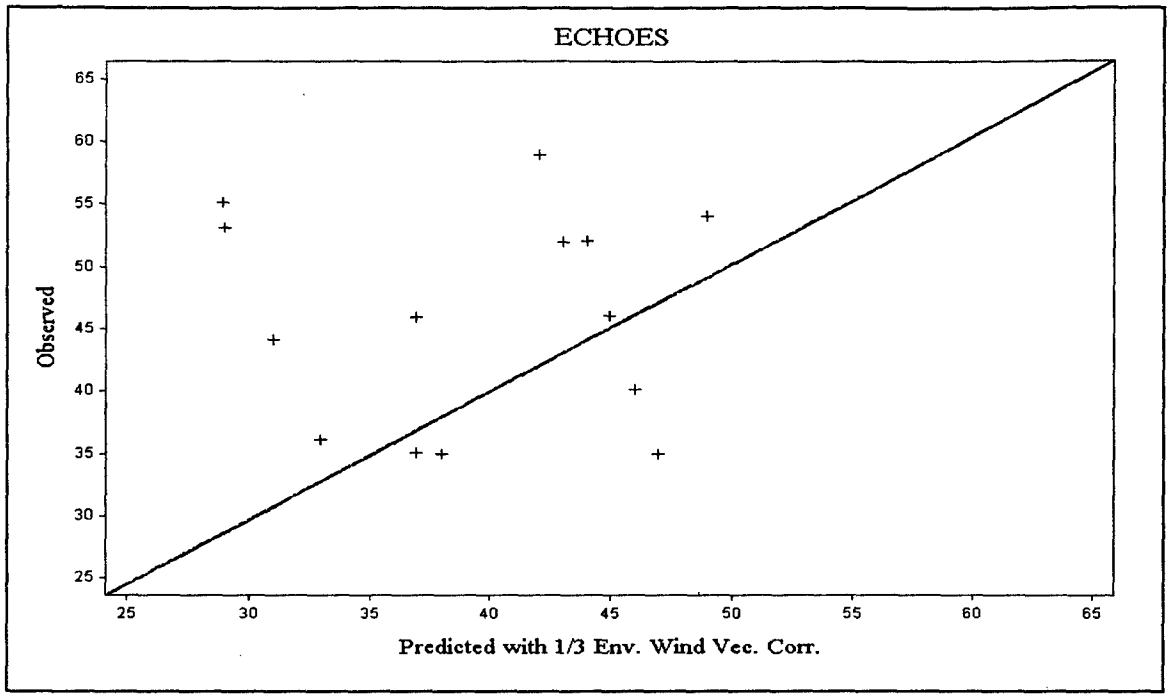

Figure 20. AWS ET/VIL WGP with 1/3 Env. Wind Vector Correction

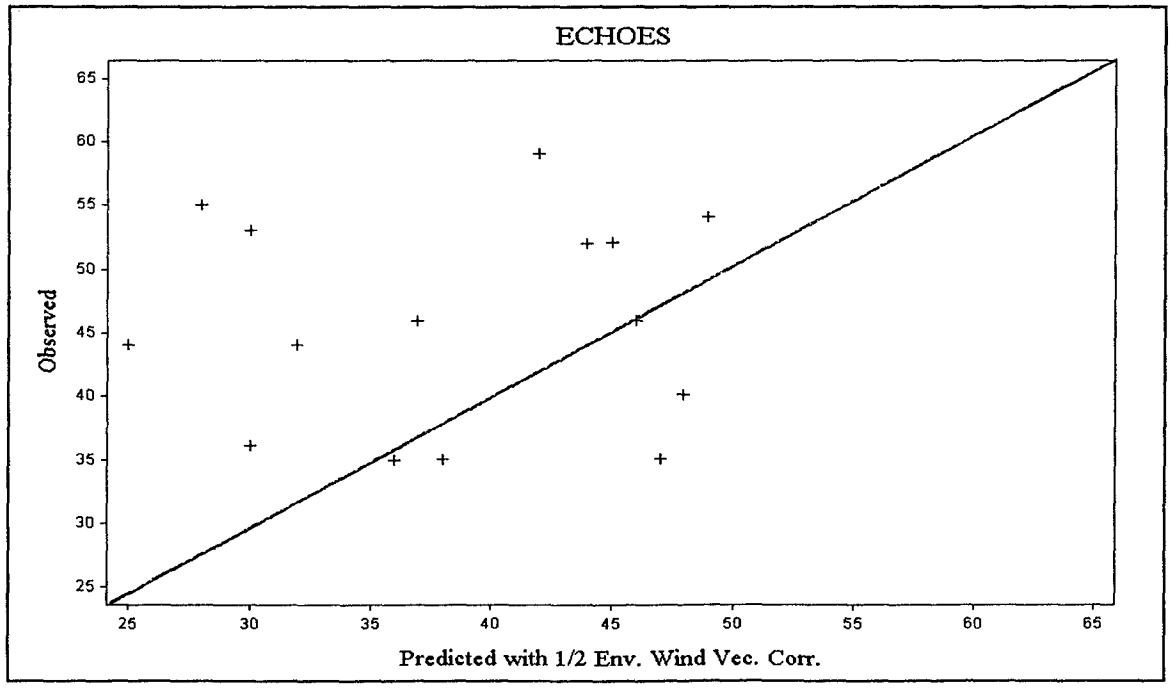

Figure 21. AWS ET/VIL WGP with 1/2 Env. Wind Vector Correction

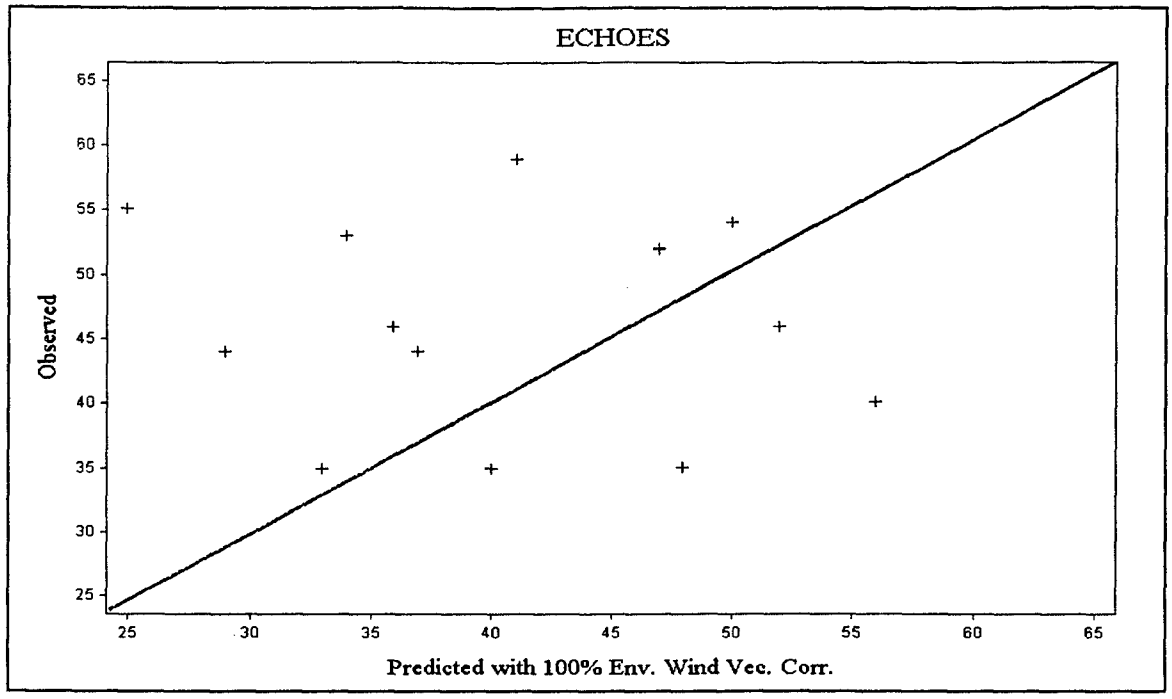

Figure 22. AWS ET/VIL WGP with 100% Env. Wind Vector Correction

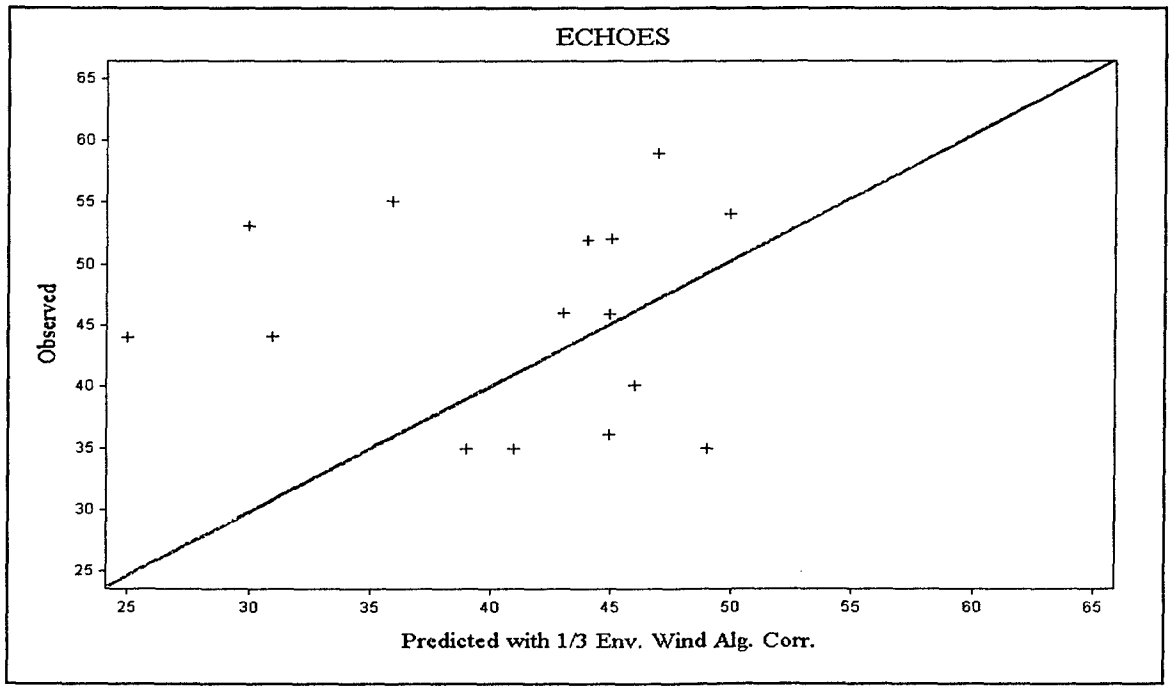

Figure 23. AWS ET/VIL WGP with 1/3 Env. Wind Algebraic Correction

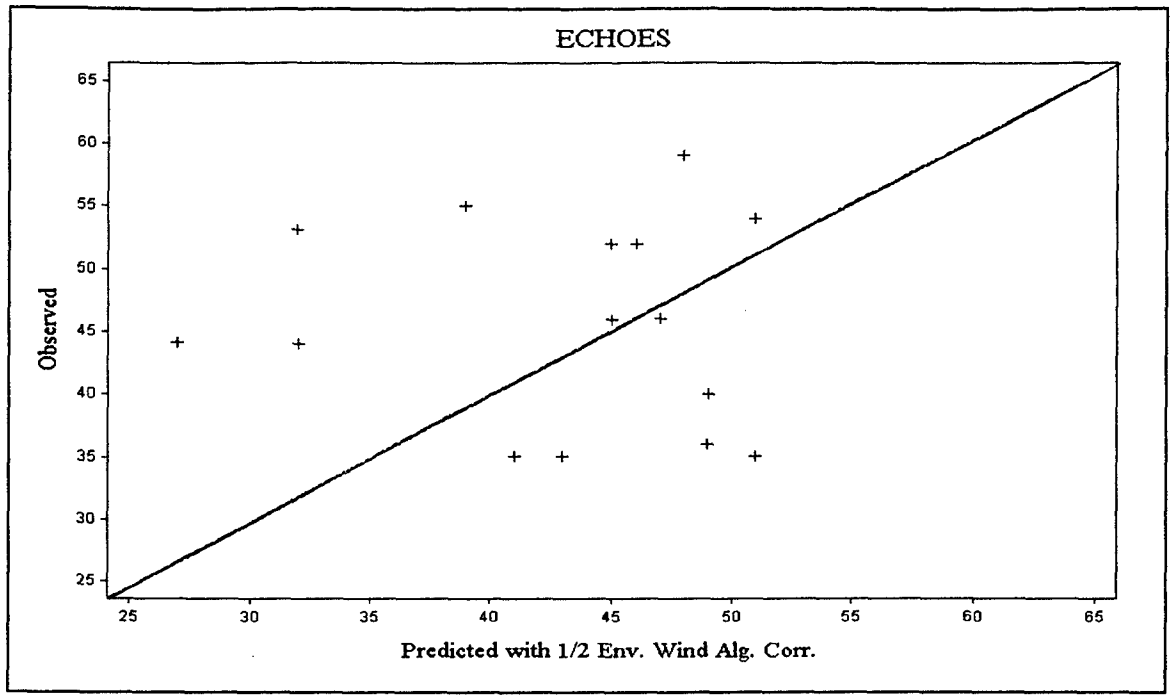

Figure 24. AWS ET/VIL WGP with 1/2 Env. Wind Algebraic Correction

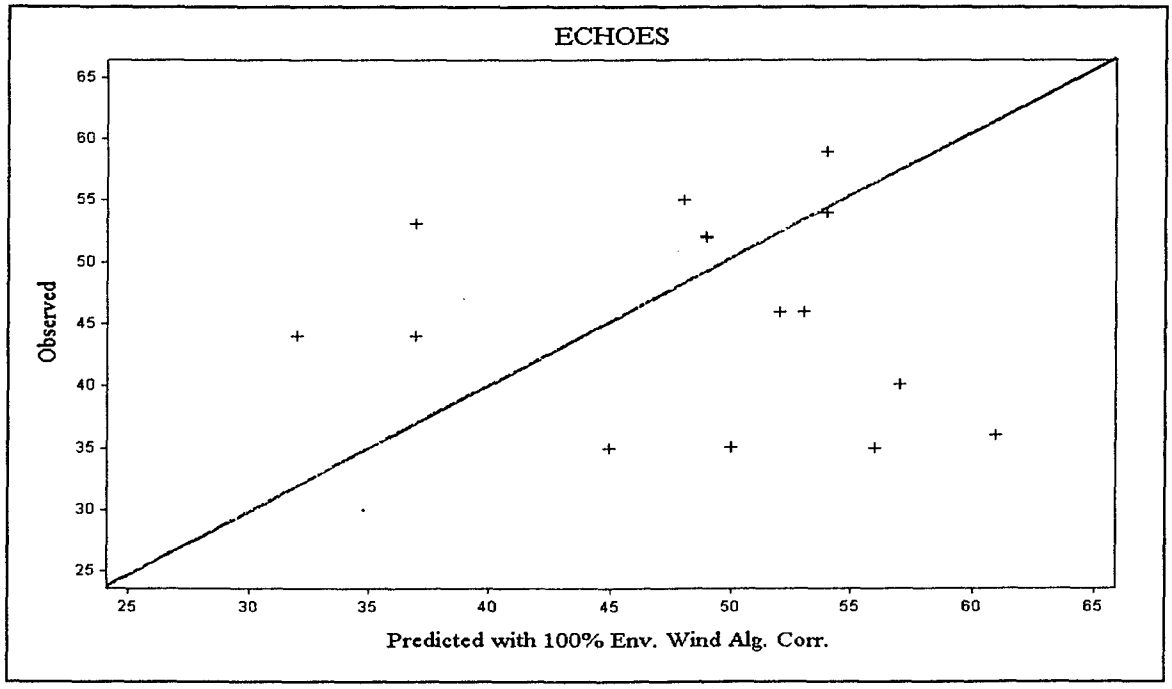

Figure 25. AWS ET/VIL WGP with 1/3 Env. Wind Algebraic Correction

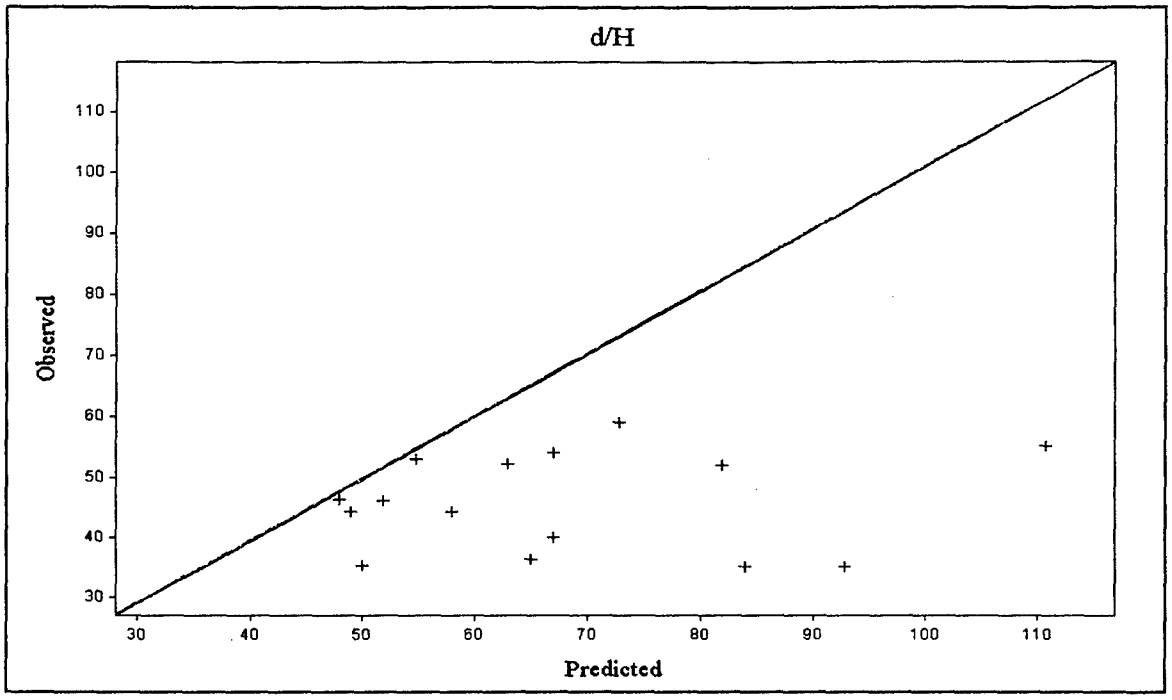

Figure 26. d/H WGP

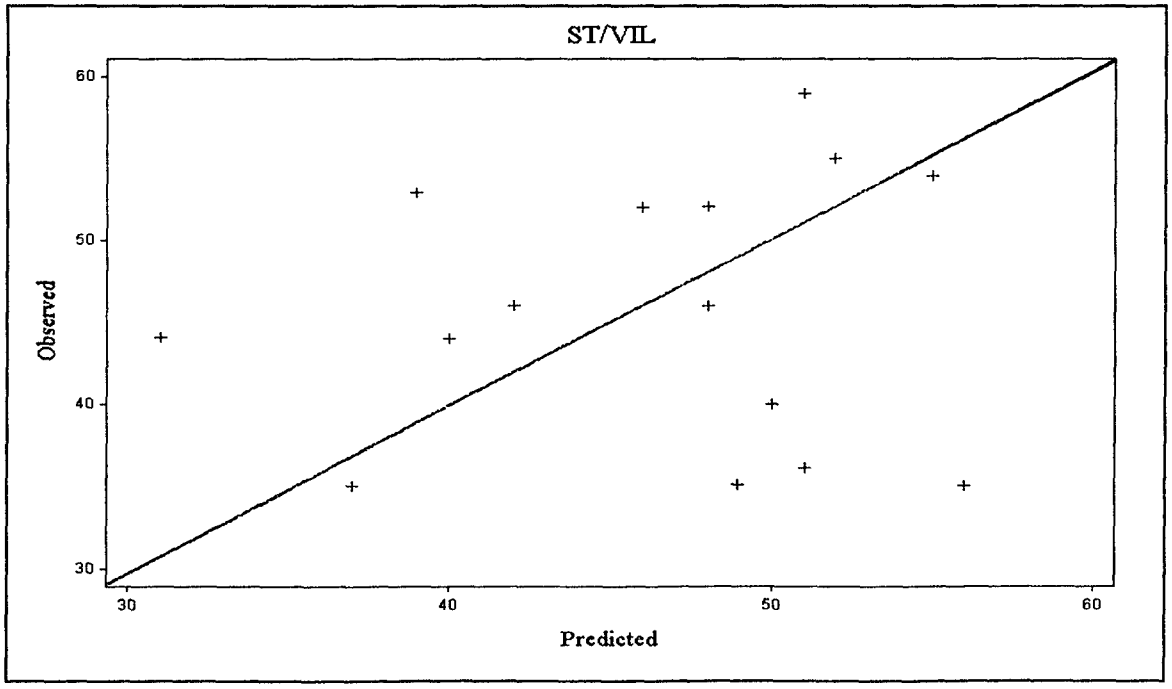

Figure 27. ST/VIL WGP

Appendix C: Data

This appendix contains the data used to calculate the WGP predictions in this thesis. The volume scan used for the calculations is in bold print. The legend is:

Date:	Date and Julian Date of event
Gust Time:	Time of peak wind as reported by WINDS
Tower Identification Number:	WINDS Tower Id Number
Gust Speed:	Peak wind as reported by WINDS
Gust Direction:	Wind direction as reported by WINDS
Time:	Time of volume scan reported by WATADS
VS:	Volume Scan number
AZRAN:	Azimuth and Range of centroid from RDA
Time until Gust:	Time between volume scan and gust time
Distance:	Distance from centroid to recording tower
ST:	Storm Top value (kft)
ET:	Echo Top value (kft)
VIL:	Vertically Integrated Liquid (kg m^{-2})
MXZ:	Maximum storm reflectivity
HMXZ:	Height of maximum storm reflectivity

Date: 94174-23Jun94

Gust Time (UTC): 2130
Tower Identification Number: 513
Tower Latitude: 28.63075 Tower Longitude: -80.70271
Gust Speed (kts): 55
Gust Direction: 315
Mean surface-5,000 ft wind: 205/17

Storm data:

Time	VS	AZRAN	Latitude	Longitude	Distance	Time until Gust
2234	210	338/34	28.63813	-80.89548	10.2	36
2239	211	341/34	28.64857	-80.86386	8.6	31
2244	212	342/33	28.63589	-80.84729	7.6	26
2249	213	344/33	28.64152	-80.82640	6.5	21
2254	214	346/32	28.63036	-80.80068	5.2	16

Parameters:

Time	ST	ET	VIL	MXZ	HMXZ
2234	46.3	44	47	67	23.4
2239	43.4	43	46	65	16.2
2244	36.2	42	48	61	15.9
2249	40.5	40	48	60	12.5
2254	30.3	48	48	61	18.8

Stewart's ET/VIL WGP Technique

Time	No Corr	1/3 Vec Corr	1/2 Vec Corr	100% Vec Corr	1/3 Alg Corr	1/2 Alg Corr	100% Alg Corr
2234	39	37	36	34	45	48	57
2239	39	38	37	34	45	48	57
2244	42	41	40	37	48	51	60
2249	44	43	42	39	50	53	62
2254	**35**	**33**	**32**	**29**	**41**	**44**	**52**

Date: 94174-23Jun94 Continued

AWS ET/VIL WGP Technique

Time	No Corr	1/3 Vec Corr	1/2 Vec Corr	100% Vec Corr	1/3 Alg Corr	1/2 Alg Corr	100% Alg Corr
2234	34	33	32	29	40	43	52
2239	35	33	32	29	40	43	52
2244	37	35	34	32	43	46	55
2249	39	37	36	34	45	48	56
2254	**31**	**29**	**28**	**25**	**36**	**39**	**48**

d/H WGP Technique

Time	Predicted
2234	**111**
2239	81
2244	61
2249	51
2254	66

ST/VIL WGP Technique

Time	Predicted
2234	36
2239	39
2244	48
2249	44
2254	**52**

Date: 94176-25Jun94

Gust Time (UTC): 2015
Tower Identification Number: 714
Tower Latitude: 28.64313 Tower Longitude: -80.74819
Gust Speed (kts): 46
Gust Direction: 330
Mean surface-5,000 ft wind: 235/15

Storm data:

Time	VS	AZRAN	Latitude	Longitude	Distance	Time until Gust
1954	53	341/33	28.63283	-80.85765	5.8	21
2000	54	347/34	28.66499	-80.79896	3.0	15
2006	55	350/34	28.67093	-80.76586	1.9	9
2012	56	352/34	28.67404	-80.74361	1.9	3

Parameters:

Time	ST	ET	VIL	MXZ	HMXZ
1954	35	35	43	59	15.7
2000	23	37	42	56	6.1
2006	38	38	44	56	13.0
2012	39	38	36	55	13.1

Stewart's ET/VIL WGP Technique

Time	No Corr	1/3 Vec Corr	1/2 Vec Corr	100% Vec Corr	1/3 Alg Corr	1/2 Alg Corr	100% Alg Corr
1954	45	44	44	43	50	52	60
2000	42	42	41	41	47	50	57
2006	**43**	**42**	**42**	**42**	**48**	**50**	**58**
2012	35	34	34	34	40	42	50

Date: 94176-25Jun94 Continued

AWS ET/VIL WGP Technique

Time	No Corr	1/3 Vec Corr	1/2 Vec Corr	100% Vec Corr	1/3 Alg Corr	1/2 Alg Corr	100% Alg Corr
1954	39	39	39	38	44	47	54
2000	37	36	36	35	42	44	52
2006	**38**	**37**	**37**	**36**	**43**	**45**	**53**
2012	31	30	30	29	36	38	46

d/H WGP Technique

Time	Predicted
1954	**52**
2000	27
2006	39
2012	36

ST/VIL WGP Technique

Time	Predicted
1954	45
2000	52
2006	**42**
2012	34

Date: 94201-20Jul94 Event #1

Gust Time (UTC): 2130
Tower Identification Number: 714
Tower Latitude: 28.64313 Tower Longitude: -80.74819
Gust Speed (kts): 36
Gust Direction: 330
Mean surface-5,000 ft wind: 200/25

Storm data:

Time	VS	AZRAN	Latitude	Longitude	Distance	Time until Gust
2052	345	339/39	28.71946	-80.91921	10.1	38
2058	346	339/40	28.73499	-80.92606	10.9	32
2104	347	336/38	28.69117	-80.94724	10.9	26
2110	348	335/37	28.67149	-80.95061	10.8	20

Parameters:

Time	ST	ET	VIL	MXZ	HMXZ
2052	42	44	59	62	15.7
2058	42	44	52	62	17.0
2104	37.8	43	43	65	18.5
2110	38	43	44	64	7.0

Stewart's ET/VIL WGP Technique

Time	No Corr	1/3 Vec Corr	1/2 Vec Corr	100% Vec Corr	1/3 Alg Corr	1/2 Alg Corr	100% Alg Corr
2052	**50**	**45**	**42**	**35**	**57**	**61**	**73**
2058	44	39	36	29	51	55	67
2104	36	31	29	22	44	48	59
2110	37	32	30	23	45	49	60

Date: 94201-20Jul94 Event #1 Continued

AWS ET/VIL WGP Technique

Time	No Corr	1/3 Vec Corr	1/2 Vec Corr	100% Vec Corr	1/3 Alg Corr	1/2 Alg Corr	100% Alg Corr
2052	**44**	**39**	**36**	**29**	**51**	**55**	**67**
2058	38	34	31	24	46	50	61
2104	32	27	24	17	39	43	55
2110	33	28	25	18	40	44	56

d/H WGP Technique

Time	Predicted
2052	65
2058	67
2104	**86**
2110	50

ST/VIL WGP Technique

Time	Predicted
2052	**51**
2058	46
2104	42
2110	43

Date: 94201-20Jul94 Event #2

Gust Time (UTC): 2230
Tower Identification Number: 110
Tower Latitude: 28.56972 Tower Longitude: -80.58641
Gust Speed (kts): 35
Gust Direction: 275
Mean surface-5,000 ft wind: 200/15

Storm data:

Time	VS	AZRAN	Latitude	Longitude	Distance	Time until Gust
2208	358	345/28	28.56369	-80.79121	10.8	22
2213	359	350/28	28.57253	-80.74599	8.4	17
2219	360	360/28	28.57965	-80.65378	3.6	11

Parameters:

Time	ST	ET	VIL	MXZ	HMXZ
2208	16.9	28	30	58	16.9
2213	34.1	29	34	56	2.0
2219	18.2	36	23	56	2.0

Stewart's ET/VIL WGP Technique

Time	No Corr	1/3 Vec Corr	1/2 Vec Corr	100% Vec Corr	1/3 Alg Corr	1/2 Alg Corr	100% Alg Corr
2208	38	40	40	42	43	45	52
2213	**41**	**43**	**43**	**45**	**46**	**48**	**55**
2219	19	20	21	23	24	26	33

AWS ET/VIL WGP Technique

Time	No Corr	1/3 Vec Corr	1/2 Vec Corr	100% Vec Corr	1/3 Alg Corr	1/2 Alg Corr	100% Alg Corr
2208	34	35	35	37	38	41	48
2213	**36**	**38**	**38**	**40**	**41**	**43**	**50**
2219	17	18	19	21	22	24	31

d/H WGP Technique

Time	Predicted
2208	**50**
2213	16
2219	16

ST/VIL WGP Technique

Time	Predicted
2208	45
2213	**37**
2219	38

Date: 94210-29Jul94

Gust Time (UTC): 2015
Tower Identification Number: 313
Tower Latitude: 28.62558 Tower Longitude: -80.65708
Gust Speed (kts): 40
Gust Direction: 220
Mean surface-5,000 ft wind: 200/15

Storm data:

Time	VS	AZRAN	Latitude	Longitude	Distance	Time until Gust
2003	104	343/28	28.55918	-80.80902	8.9	12
2008	105	344/29	28.57751	-80.80538	8.3	7
2013	106	343/30	28.59102	-80.82016	8.8	2

Parameters:

Time	ST	ET	VIL	MXZ	HMXZ
2003	42.9	46	58	61	19.7
2008	42.5	48	50	60	17.5
2013	40.4	47	43	63	14.5

Stewart's ET/VIL WGP Technique

Time	No Corr	1/3 Vec Corr	1/2 Vec Corr	100% Vec Corr	1/3 Alg Corr	1/2 Alg Corr	100% Alg Corr
2003	**47**	**51**	**54**	**61**	**52**	**54**	**62**
2008	37	42	44	51	42	44	52
2013	30	35	37	45	35	38	45

AWS ET/VIL WGP Technique

Time	No Corr	1/3 Vec Corr	1/2 Vec Corr	100% Vec Corr	1/3 Alg Corr	1/2 Alg Corr	100% Alg Corr
2003	**41**	**46**	**48**	**56**	**46**	**49**	**57**
2008	32	37	40	47	38	40	48
2013	27	32	34	42	32	35	43

d/H WGP Technique

Time	Predicted
2003	67
2008	59
2013	**67**

ST/VIL WGP Technique

Time	Predicted
2003	**50**
2008	44
2013	39

Date: 96226-14Aug96

Gust Time (UTC): 2050
Tower Identification Number: 300
Tower Latitude: 28.40479 Tower Longitude: -80.65192
Gust Speed (kts): 35
Gust Direction: 290
Mean surface-5,000 ft wind: 215/10

Storm data:

Time	VS	AZRAN	Latitude	Longitude	Distance	Time until Gust
2034	135	356/16	28.37913	-80.67491	2.0	16
2039	136	357/18	28.41268	-80.67162	1.1	11
2044	137	357/18	28.41268	-80.67162	1.1	6
2049	138	357/18	28.41268	-80.67162	1.1	1

Parameters:

Time	ST	ET	VIL	MXZ	HMXZ
2034	34	39	57	67	16.2
2039	35	39	54	64	14.4
2044	34	39	48	63	10.5
2049	34	39	42	61	12.0

Stewart's ET/VIL WGP Technique

Time	No Corr	1/3 Vec Corr	1/2 Vec Corr	100% Vec Corr	1/3 Alg Corr	1/2 Alg Corr	100% Alg Corr
2034	**53**	**53**	**54**	**55**	**56**	**58**	**63**
2039	50	51	51	53	54	55	60
2044	45	46	47	48	49	50	55
2049	40	41	41	42	43	45	50

Date: 96226-14Aug96 Continued

AWS ET/VIL WGP Technique

Time	No Corr	1/3 Vec Corr	1/2 Vec Corr	100% Vec Corr	1/3 Alg Corr	1/2 Alg Corr	100% Alg Corr
2034	**46**	**47**	**47**	**48**	**49**	**51**	**56**
2039	44	45	45	46	47	49	54
2044	40	41	41	42	43	45	50
2049	35	36	36	37	38	40	45

d/H WGP Technique

Time	Predicted
2034	**93**
2039	71
2044	57
2049	53

ST/VIL WGP Technique

Time	Predicted
2034	**56**
2039	54
2044	49
2049	44

Date: 97170-19Jun97

Gust Time (UTC): 2005
Tower Identification Number: 19
Tower Latitude: 28.74348 Tower Longitude: -80.70053
Gust Speed (kts): 59
Gust Direction: 360
Mean surface-5,000 ft wind: 260/10

Storm data:

Time	VS	AZRAN	Latitude	Longitude	Distance	Time until Gust
1945	321	353/44	28.84064	-80.75574	6.5	20
1950	322	353/43	28.82411	-80.7534	5.6	15
1955	323	353/42	28.80758	-80.75107	4.7	10
2000	324	350/40	28.76933	-80.78576	4.7	5

Parameters:

Time	ST	ET	VIL	MXZ	HMXZ
1945	43	50	47	59	17.0
1950	46	47	62	60	28.5
1955	45	47	62	58	20.2
2000	43	47	45	57	15.8

Stewart's ET/VIL WGP Technique

Time	No Corr	1/3 Vec Corr	1/2 Vec Corr	100% Vec Corr	1/3 Alg Corr	1/2 Alg Corr	100% Alg Corr
1945	30	30	29	28	34	36	41
1950	49	48	48	47	53	54	60
1955	**49**	**48**	**48**	**47**	**53**	**54**	**60**
2000	33	32	32	31	36	38	44

Date: 97170-19Jun97 Continued

AWS ET/VIL WGP Technique

Time	No Corr	1/3 Vec Corr	1/2 Vec Corr	100% Vec Corr	1/3 Alg Corr	1/2 Alg Corr	100% Alg Corr
1945	27	26	26	25	30	32	38
1950	43	42	42	41	47	48	54
1955	**43**	**42**	**42**	**41**	**47**	**48**	**54**
2000	29	28	28	27	33	34	40

d/H WGP Technique

Time	Predicted
1945	54
1950	**73**
1955	54
2000	45

ST/VIL WGP Technique

Time	Predicted
1945	40
1950	50
1955	**51**
2000	38

Date: 97210-29Jul97 Event #1

Gust Time (UTC): 2130
Tower Identification Number: 421
Tower Latitude: 28.77547 Tower Longitude: -80.80433
Gust Speed (kts): 44
Gust Direction: 155
Mean surface-5,000 ft wind: 160/10

Storm data:

Time	VS	AZRAN	Latitude	Longitude	Distance	Time until Gust
2110	85	347/37	28.71366	-80.81184	3.7	20
2116	86	348/43	28.81373	-80.82372	2.5	14
2121	87	347/39	28.74611	-80.82044	2.0	9
2126	88	348/39	28.74858	-80.80782	1.6	4

Parameters:

Time	ST	ET	VIL	MXZ	HMXZ
2110	36.3	43	39	61	14.6
2116	36.6	43	36	58	14.8
2121	16.3	38	26	56	11.2
2126	31.3	38	17	52	3.2

Stewart's ET/VIL WGP Technique

Time	No Corr	1/3 Vec Corr	1/2 Vec Corr	100% Vec Corr	1/3 Alg Corr	1/2 Alg Corr	100% Alg Corr
2110	**32**	**35**	**36**	**41**	**35**	**36**	**41**
2116	28	31	32	37	31	32	37
2121	21	24	25	30	24	25	30
2126	N/A	N/A	N/A	N/A	N/A	N/A	N/A

Date: 97210-29Jul97 Event #1 Continued

AWS ET/VIL WGP Technique

Time	No Corr	1/3 Vec Corr	1/2 Vec Corr	100% Vec Corr	1/3 Alg Corr	1/2 Alg Corr	100% Alg Corr
2110	**28**	**31**	**32**	**37**	**31**	**32**	**37**
2116	24	27	29	33	27	29	33
2121	18	21	23	27	21	23	27
2126	N/A	N/A	N/A	N/A	N/A	N/A	N/A

d/H WGP Technique

Time	Predicted
2110	**58**
2116	47
2121	36
2126	15

ST/VIL WGP Technique

Time	Predicted
2110	**40**
2116	36
2121	42
2126	16

Date: 97210-29Jul97 Event #2

Gust Time (UTC): 2310
Tower Identification Number: 22
Tower Latitude: 28.79747 Tower Longitude: -80.73780
Gust Speed (kts): 53
Gust Direction: 220
Mean surface-5,000 ft wind: 170/10

Storm data:

Time	VS	AZRAN	Latitude	Longitude	Distance	Time until Gust
2251	105	348/37	28.71600	-80.79987	5.9	19
2256	106	351/38	28.73836	-80.76670	3.9	14
2301	107	353/38	28.74146	-80.74175	3.4	9
2306	108	355/39	28.76037	-80.71836	2.5	4

Parameters:

Time	ST	ET	VIL	MXZ	HMXZ
2251	34.5	43	33	59	17.3
2256	30.7	37	35	57	18.5
2301	35.5	42	37	58	15.0
2306	35.7	43	28	55	7.4

Stewart's ET/VIL WGP Technique

Time	No Corr	1/3 Vec Corr	1/2 Vec Corr	100% Vec Corr	1/3 Alg Corr	1/2 Alg Corr	100% Alg Corr
2251	23	25	27	30	27	28	33
2256	35	37	38	42	38	40	45
2301	**31**	**33**	**34**	**37**	**34**	**36**	**41**
2306	13	15	16	20	16	18	23

Date: 97210-29Jul97 Event #2 Continued

AWS ET/VIL WGP Technique

Time	No Corr	1/3 Vec Corr	1/2 Vec Corr	100% Vec Corr	1/3 Alg Corr	1/2 Alg Corr	100% Alg Corr
2251	21	23	24	27	24	26	31
2256	31	33	34	37	34	36	41
2301	**27**	**29**	**30**	**34**	**30**	**32**	**37**
2306	12	14	15	18	15	17	22

d/H WGP Technique

Time	Predicted
2251	**55**
2256	48
2301	48
2306	28

ST/VIL WGP Technique

Time	Predicted
2251	36
2256	41
2301	**39**
2306	28

Date: 97232-20Aug97 Event #1

Gust Time (UTC): 2150
Tower Identification Number: 513
Tower Latitude: 28.63075 Tower Longitude: -80.70271
Gust Speed (kts): 44
Gust Direction: 325
Mean surface-5,000 ft wind: 275/10

Storm data:

Time	VS	AZRAN	Latitude	Longitude	Distance	Time until Gust
2133	264	350/34	28.67093	-80.76586	4.1	17
2138	265	350/34	28.67093	-80.76586	4.1	12
2143	266	352/34	28.67404	-80.74361	3.4	7

Parameters:

Time	ST	ET	VIL	MXZ	HMXZ
2133	46.8	46	39	59	13.4
2138	44.3	48	40	57	16.1
2143	44.0	45	31	56	17.0

Stewart's ET/VIL WGP Technique

Time	No Corr	1/3 Vec Corr	1/2 Vec Corr	100% Vec Corr	1/3 Alg Corr	1/2 Alg Corr	100% Alg Corr
2133	27	29	30	34	30	32	38
2138	**24**	**27**	**28**	**31**	**28**	**30**	**35**
2143	14	16	18	21	18	19	25

AWS ET/VIL WGP Technique

Time	No Corr	1/3 Vec Corr	1/2 Vec Corr	100% Vec Corr	1/3 Alg Corr	1/2 Alg Corr	100% Alg Corr
2133	24	26	27	31	27	29	35
2138	**21**	**24**	**25**	**29**	**25**	**27**	**32**
2143	12	15	16	20	16	18	23

d/H WGP Technique

Time	Predicted
2133	**49**
2138	46
2143	43

ST/VIL WGP Technique

Time	Predicted
2133	25
2138	**31**
2143	17

Date: 97232-20Aug97 Event #2

Gust Time (UTC): 2220
Tower Identification Number: 300
Tower Latitude: 28.40479 Tower Longitude: -80.65192
Gust Speed (kts): 46
Gust Direction: 295
Mean surface-5,000 ft wind: 310/10

Storm data:

Time	VS	AZRAN	Latitude	Longitude	Distance	Time until Gust
2159	269	347/19	28.42161	-80.73472	4.5	21
2204	270	349/18	28.40757	-80.71882	3.5	16
2209	271	349/17	28.39122	-80.71519	3.4	11

Parameters:

Time	ST	ET	VIL	MXZ	HMXZ
2159	40.3	41	52	59	12.9
2204	37.8	41	50	57	16.3
2209	37.9	40	38	58	13.7

Stewart's ET/VIL WGP Technique

Time	No Corr	1/3 Vec Corr	1/2 Vec Corr	100% Vec Corr	1/3 Alg Corr	1/2 Alg Corr	100% Alg Corr
2159	**47**	**50**	**52**	**58**	**51**	**52**	**58**
2204	45	49	51	56	49	51	56
2209	35	38	40	45	38	40	46

AWS ET/VIL WGP Technique

Time	No Corr	1/3 Vec Corr	1/2 Vec Corr	100% Vec Corr	1/3 Alg Corr	1/2 Alg Corr	100% Alg Corr
2159	**41**	**45**	**46**	**52**	**45**	**47**	**52**
2204	40	43	45	50	43	45	51
2209	30	34	36	41	34	36	41

d/H WGP Technique

Time	Predicted
2159	**48**
2204	46
2209	46

ST/VIL WGP Technique

Time	Predicted
2159	**48**
2204	48
2209	37

Date: 98199-18Jul98

Gust Time (UTC): 2155
Tower Identification Number: 1007
Tower Latitude: 28.52718 Tower Longitude: -80.77420
Gust Speed (kts): 35
Gust Direction: 220
Mean surface-5,000 ft wind: 210/05

Storm data:

Time	VS	AZRAN	Latitude	Longitude	Distance	Time until Gust
2130	2	334/25	28.48738	-80.86146	5.2	25
2135	3	335/26	28.50561	-80.86204	4.8	20
2140	4	335/26	28.50561	-80.86204	4.8	15
2145	5	335/26	28.50561	-80.86204	4.8	10
2150	6	336/27	28.52396	-80.86196	4.6	5

Parameters:

Time	ST	ET	VIL	MXZ	HMXZ
2130	38.0	40	42	61	21.2
2135	38.1	43	51	65	17.5
2140	38.0	43	47	62	12.3
2145	43.1	43	44	60	7.4
2150	37	43	28	59	9.9

Stewart's ET/VIL WGP Technique

Time	No Corr	1/3 Vec Corr	1/2 Vec Corr	100% Vec Corr	1/3 Alg Corr	1/2 Alg Corr	100% Alg Corr
2130	39	41	42	45	41	42	45
2135	**44**	**46**	**47**	**50**	**46**	**47**	**50**
2140	40	42	43	46	42	43	46
2145	37	39	40	43	39	40	43
2150	12	14	15	18	14	15	18

Date: 98199-18Jul98 Continued

AWS ET/VIL WGP Technique

Time	No Corr	1/3 Vec Corr	1/2 Vec Corr	100% Vec Corr	1/3 Alg Corr	1/2 Alg Corr	100% Alg Corr
2130	34	36	37	40	36	37	40
2135	**39**	**41**	**42**	**45**	**41**	**42**	**45**
2140	35	37	38	41	37	38	41
2145	33	35	36	39	35	36	39
2150	11	13	14	17	13	14	17

d/H WGP Technique

Time	Predicted
2130	69
2135	**84**
2140	58
2145	39
2150	42

ST/VIL WGP Technique

Time	Predicted
2130	41
2135	**49**
2140	46
2145	37
2150	26

Date: 98209-28Jul98 Event #1

Gust Time (UTC): 2130
Tower Identification Number: 22
Tower Latitude: 28.79747 Tower Longitude: -80.73780
Gust Speed (kts): 52
Gust Direction: 320
Mean surface-5,000 ft wind: 275/10

Storm data:

Time	VS	AZRAN	Latitude	Longitude	Distance	Time until Gust
2101	50	347/44	28.82722	-80.84195	5.8	29
2106	51	347/43	28.811	-80.83764	5.3	24
2111	52	348/42	28.79744	-80.81974	4.3	19
2116	53	350/43	28.81853	-80.79572	3.3	14

Parameters:

Time	ST	ET	VIL	MXZ	HMXZ
2101	46.5	46	58	63	12.8
2106	39.7	45	44	61	12.4
2111	34.4	39	38	60	3.5
2116	34.9	30	40	59	12

Stewart's ET/VIL WGP Technique

Time	No Corr	1/3 Vec Corr	1/2 Vec Corr	100% Vec Corr	1/3 Alg Corr	1/2 Alg Corr	100% Alg Corr
2101	**47**	**49**	**50**	**52**	**49**	**51**	**55**
2106	35	37	38	40	37	39	43
2111	36	38	39	42	39	40	44
2116	46	48	49	52	49	50	54

Date: 98209-28Jul98 Event #1 Continued

AWS ET/VIL WGP Technique

Time	No Corr	1/3 Vec Corr	1/2 Vec Corr	100% Vec Corr	1/3 Alg Corr	1/2 Alg Corr	100% Alg Corr
2101	**41**	**43**	**44**	**47**	**44**	**45**	**49**
2106	30	32	33	36	33	34	38
2111	31	33	34	37	34	35	39
2116	40	42	43	46	43	44	48

d/H WGP Technique

Time	Predicted
2101	**63**
2106	54
2111	27
2116	46

ST/VIL WGP Technique

Time	Predicted
2101	**46**
2106	41
2111	41
2116	42

Date: 98209-28Jul98 Event #2

Gust Time (UTC): 2200
Tower Identification Number: 397
Tower Latitude: 28.62941 Tower Longitude: -80.62353
Gust Speed (kts): 52
Gust Direction: 315
Mean surface-5,000 ft wind: 275/05

Storm data:

Time	VS	AZRAN	Latitude	Longitude	Distance	Time until Gust
2131	56	350/34	28.67093	-80.76586	7.9	29
2136	57	351/34	28.67257	-80.75475	7.4	24
2141	58	356/33	28.66158	-80.69747	4.3	19
2146	59	357/34	28.6788	-80.68756	4.5	14
2151	60	359/32	28.64619	-80.66438	2.4	9

Parameters:

Time	ST	ET	VIL	MXZ	HMXZ
2131	41.3	47	54	64	19.2
2136	34.2	49	55	62	15.4
2141	48.6	48	63	62	26.6
2146	47	46	48	62	21.5
2151	33.1	40	44	62	8.9

Stewart's ET/VIL WGP Technique

Time	No Corr	1/3 Vec Corr	1/2 Vec Corr	100% Vec Corr	1/3 Alg Corr	1/2 Alg Corr	100% Alg Corr
2131	42	44	44	47	44	45	48
2136	41	42	43	45	43	44	47
2141	**49**	**50**	**51**	**53**	**51**	**52**	**55**
2146	38	39	40	42	40	41	44
2151	41	42	43	45	43	44	47

Date: 98209-28Jul98 Event #2 Continued

AWS ET/VIL WGP Technique

Time	No Corr	1/3 Vec Corr	1/2 Vec Corr	100% Vec Corr	1/3 Alg Corr	1/2 Alg Corr	100% Alg Corr
2131	37	39	39	42	39	40	43
2136	36	37	38	40	38	39	42
2141	**43**	**44**	**45**	**47**	**45**	**46**	**49**
2146	33	35	35	38	35	36	39
2151	36	37	38	40	38	39	42

d/H WGP Technique

Time	Predicted
2131	**82**
2136	64
2141	82
2146	75
2151	49

ST/VIL WGP Technique

Time	Predicted
2131	48
2136	55
2141	**48**
2146	36
2151	47

Date: 98226-14Aug98

Gust Time (UTC): 1935
Tower Identification Number: 1007
Tower Latitude: 28.52718 Tower Longitude: -80.77420
Gust Speed (kts): 54
Gust Direction: 350
Mean surface-5,000 ft wind: 270/05

Storm data:

Time	VS	AZRAN	Latitude	Longitude	Distance	Time until Gust
1908	41	344/31	28.60952	-80.81589	5.4	27
1913	42	344/30	28.59351	-80.81064	4.4	22
1918	43	344/29	28.57751	-80.80538	3.4	17
1923	44	345/29	28.57977	-80.79614	3.4	12
1928	45	347/28	28.56764	-80.77323	2.4	7

Parameters:

Time	ST	ET	VIL	MXZ	HMXZ
1908	39.1	45	51	62	28
1913	42.9	50	69	61	31.9
1918	50.6	50	75	62	23.5
1923	26.1	45	64	65	10.9
1928	46.4	46	47	60	7.6

Stewart's ET/VIL WGP Technique

Time	No Corr	1/3 Vec Corr	1/2 Vec Corr	100% Vec Corr	1/3 Alg Corr	1/2 Alg Corr	100% Alg Corr
1908	42	42	42	43	43	44	47
1913	51	52	52	52	53	54	56
1918	**56**	**56**	**56**	**56**	**57**	**58**	**61**
1923	52	53	53	53	54	55	57
1928	37	37	37	37	38	39	42

Date: 98226-14Aug98 Continued

AWS ET/VIL WGP Technique

Time	No Corr	1/3 Vec Corr	1/2 Vec Corr	100% Vec Corr	1/3 Alg Corr	1/2 Alg Corr	100% Alg Corr
1908	37	37	37	38	38	39	42
1913	45	45	45	46	47	47	50
1918	**49**	**49**	**49**	**50**	**50**	**51**	**54**
1923	46	46	46	47	48	48	51
1928	32	32	33	33	34	35	37

d/H WGP Technique

Time	Predicted
1908	84
1913	83
1918	78
1923	**67**
1928	40

ST/VIL WGP Technique

Time	Predicted
1908	48
1913	58
1918	**55**
1923	65
1928	36

Appendix D: Mathcad© Templates

latlon2azran.mcd

This template is used to calculate distances between two latitude and longitude points. It works properly for the first and second mathematical quadrants. That is θ1 and ϕ1 should be chosen such that θ2 and ϕ2 are in the first or second quadrant. It also calculates the azimuth from point 1 to point 2. These equations are taken from the book Distance and Azimuth Computations with Tables by Harry C. Carver, Edward Brothers Inc, 1954

ORIGIN≡1

Constants used by template:

$Rad := 6370.939 \cdot km$ $nm := 1852 \cdot m$

Input data:

$\theta_1 := 28.92891 \cdot deg$ $\theta_2 := 28.92891 \cdot deg$

$\phi_1 := -80.68632 \cdot deg$ $\phi_2 := -80.68632 \cdot deg$

This calculates the great circle distance between the two lat/lon points

$$D := acos\left(sin\left(\theta_1\right) \cdot sin\left(\theta_2\right) + cos\left(\theta_1\right) \cdot cos\left(\theta_2\right) \cdot cos\left(\phi_2 - \phi_1\right)\right)$$

$Dist := D \cdot Rad$ $Dist = 0 \cdot nm$

This calculates the angles between the two points.

$$\psi := asin\left(\frac{cos\left(\theta_2\right) \cdot sin\left(\phi_2 - \phi_1\right)}{sin(D)}\right) \qquad \psi = 0 \cdot deg$$

Summary data:

Range from point 1 to point 2: $Dist = 0 \cdot nm$

Azimuth to point 2 from point 1: $\psi = 0 \cdot deg$ Add 360 to negative values

azran2latlon.mcd

This part allows the calculation of latitude and longitude given azimuth and range

$MLBLAT := 28.11329 \cdot deg$

$MLBLON := -80.65378 \cdot deg$

$\theta_1 := MLBLAT \qquad \theta_2 := 28.5 \cdot deg$

$\phi_1 := MLBLON \qquad \phi_2 := -80 \cdot deg \qquad nm := 1852 \cdot m \qquad Rad := 6370.939 \cdot km$

$RAN := 46 \cdot nm \qquad AZ := (360 - 360) \cdot deg \qquad \psi := AZ \qquad D := \frac{RAN}{Rad} \qquad D = 0.013$

Given

$$D = \operatorname{acos}\left(\sin(\theta_1)\cdot\sin(\theta_2) + \cos(\theta_1)\cdot\cos(\theta_2)\cdot\cos(\phi_2 - \phi_1)\right)$$

This calculates the angles between the two points.

$$\psi = \operatorname{asin}\left(\frac{\cos(\theta_2)\cdot\sin(\phi_2 - \phi_1)}{\sin(D)}\right)$$

$ans := Find(\theta_2, \phi_2)$

$$ans = \begin{bmatrix} 28.87945 \\ -80.65378 \end{bmatrix} \cdot deg$$

Thetaecalc.mcd

This template reads in the sorted KXMR soundings: sorted such that the columns are arranged as follows:
first row is hour, month, day, year, and three filler zeros.
other rows height(ft), wind dir, wind sp, temp, td, pressure, RH.
It then converts column order to that read by SHARP
It then calculates theta-e using equations from AWS/TR-83/001
It then creates a file, with necessary filler lines, that can be plotted by SHARP
It also creates a file with the theta-e values for future reference.
Finally, it plots theta-e.

ORIGIN≡1 in := READPRN("i:\KXMRSoundings\sorted\25Jun9410z.txt")

rows(in) = i := 1 .. 40

Converts input to Sharp format:

$$out_{i,1} := in_{i+1,6} \quad out_{i,2} := in_{i+1,1} \quad out_{i,3} := in_{i+1,4} \quad out_{i,4} := in_{i+1,5}$$
$$out_{i,5} := in_{i+1,5} \quad out_{i,6} := in_{i+1,2} \quad out_{i,7} := in_{i+1,3}$$

Used later to calculate theta-e:

$$T_i := in_{i+1,4} + 273.16 \qquad P_i := in_{i+1,6} \qquad k := 0.2854$$

Calculates T_{LCL}

$$T_{LCL_i} := in_{i+1,5} - \left(0.212 + 0.001571 \cdot in_{i+1,5} - 0.000436 \cdot in_{i+1,4}\right) \cdot \left(in_{i+1,4} - in_{i+1,5}\right) + 273.16$$

Calculates vapor pressure, e:

$$vp_i := 6.11 \cdot 10^{\left(\frac{7.5 \cdot in_{i+1,5}}{in_{i+1,5} + 237.3}\right)}$$

Calculates mixing ratio, w,:

$$w_i := 1000 \cdot .622 \cdot \frac{vp_i}{\left(P_i - vp_i\right)}$$

Calculates theta-e

$$\theta e_i := \left(T_i\right) \cdot \left(\frac{1000}{P_i}\right)^{k \cdot \left(1 - 0.28 \cdot 10^{-3} \cdot w_i\right)} \cdot e^{\left(\frac{3.376}{T_{LCL_i}} - 0.00254\right) \cdot w_i \cdot \left(1 + 0.81 \cdot 10^{-3} \cdot w_i\right)}$$

$$out_{i,5} := \theta e_i$$

$$top := \begin{bmatrix} 0 & 0 & 0 & 0 & 0 & 0 & 0 \\ 0 & 0 & 0 & 0 & 0 & 0 & 0 \\ 0 & 0 & 0 & 0 & 0 & 0 & 0 \\ 0 & 0 & 0 & 0 & 0 & 0 & 0 \\ 0 & 0 & 0 & 0 & 0 & 0 & 0 \\ 0 & 0 & 0 & 0 & 0 & 0 & 0 \\ 0 & 0 & 0 & 0 & 0 & 0 & 0 \end{bmatrix} \qquad j := 1 .. 7$$

$$output := stack\left(date^{T}, stack(top, out)\right)$$

Produces matrix with H, P, theta-e

$$\theta eout_{i,1} := in_{i+1,1} \qquad \theta eout_{i,2} := in_{i+1,6} \qquad \theta eout_{i,3} := \theta e_{i}$$

WRITEPRN("i:\KXMRSoundings\thetae\25Jun9410zte.dat") := θeout

WRITEPRN("i:\KXMRSoundings\converted\25Jun9410z.dat") := output

$$j := 1 .. rows(out)$$

$$\left(out^{\langle 1 \rangle}\right)_{j}$$

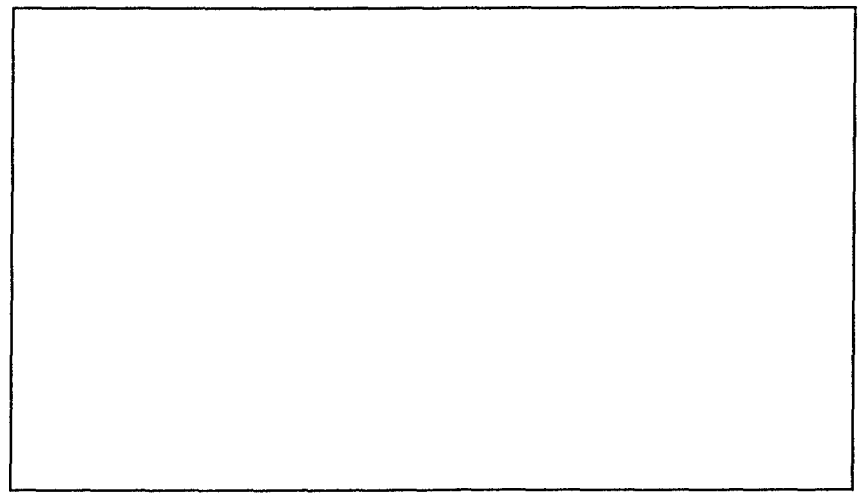

$$(\theta e)_{j}$$

Bibliography

Atkins, NolanT. and Roger M. Wakimoto. "Wet Microburst Activity Over the Southeastern United States: Implications for Forecasting," Weather and Forecasting, **6**: 470-482 (December 1991)

Air Education and Training Command. Radar Theory/PUP Operator (Study Guide KWXR-2001)., Keesler AFB, MS., 1993.

Air Weather Service (AWS). ECHOES: Operational Use of Vertically Integrated Liquid (VIL)., No. 16. Scott AFB: Air Weather Service, 1996.

Bolton, David. "The Computation of Equivalent Potential Temperature," Monthly Weather Review, **108:** 1046-1053 (July 1990)

Carver, Harry C. Distance and Azimuth Computations with Tables. Ann Arbor: Edwards Brothers, Inc., 1954.

Department of Commerce. Doppler Radar Meteorological Observations Part B. Federal Meteorological Handbook 11. Washington: OFCM, June 1990.

Department of Commerce. Doppler Radar Meteorological Observations Part C. Federal Meteorological Handbook 11 Washington: OFCM, February 1991.

Emanuel, Kerry A. "A Similarity Theory for Unsaturated Downdrafts within Clouds," Journal of the Atmospheric Sciences, **36:** 2462-2478 (August 1981)

Frazier, Mark. "The Prediction of Thunderstorm Wind Gusts Based on Vertically Integrated Water Content and Storm Echo Tops", Eastern Region Technical Attachment, No 94-7B, 1994.

Fujita, Theodore T. The Downburst: Microburst and Macroburst. Chicago: University of Chicago Press, 1985.

Greene, Douglas. R. and Robert A. Clark. "Vertically Integrated Liquid Water—A New Analysis Tool," Monthly Weather Review, **100:** 548-552.

Huschke, Ralph E. (Ed.). Glossary of Meteorology. Boston: American Meteorological Society, 1959.

National Oceanic and Atmospheric Administration. Daily Weather Maps. 1 June 1994-27 August 1997. Washington: Department of Commerce, 1994-1997

Roeder, William. Chief Staff Meteorologist, 45th Weather Squadron, Patrick AFB, FL. Personal Correspondences. July - December 1998.

Roeder, William. "An Update to an Overview of Wet Microburst Forecasting at 45th Weather Squadron," Proceedings of the NEXRAD OSF 2nd Pulse Storm Downburst Prediction Workshop. (December, 1998)

Srivastava, R. C. "A Simple Model of Evaporatively Driven Downdraft: Application to Microburst Downdraft," Journal of the Atmospheric Sciences, **42:** 1004-1023 (May 85)

Stewart, Stacy R. The Prediction of Pulse-Type Thunderstorm Gusts Using Vertically Integrated Liquid Water Content (VIL) and the Cloud Top Penetrative Downdraft Mechanism. NOAA Tech. Memo, NWS SR-136, (October 1991)

---------. An Empirical Forecasting Technique for Predicting Pulse-Type Thunderstorm Gusts Using Radar Derived Vertically Integrated Liquid (VIL) and the Penetrative Downdraft Mechanism. MS non-thesis, University of Oklahoma, 1992.

---------. "Wet Microbursts—Predicting Peak Wind Gusts Associated with Summertime Pulse-type Thunderstorms," Proceedings of the 15th Conference on Weather Analysis and Forecasting. 324-327. Boston: American Meteorological Society, 1996.

---------. Meteorologist Instructor, NEXRAD Operational Support Facility, Norman, OK. Personal Correspondences. September-December 1998.

Wheeler, Mark. Analysis and Review of Downrush Wind Events on 16 August 1994. AMU Memorandum, (November 1994)

Wilks, Daniel S. Statistical Methods in the Atmospheric Sciences. Boston: Academic Press, 1995.

REPORT DOCUMENTATION PAGE

Form Approved
OMB No. 0704-0188

1. AGENCY USE ONLY *(Leave blank)*	2. REPORT DATE	3. REPORT TYPE AND DATES COVERED
	March 1999	Master's Thesis

4. TITLE AND SUBTITLE
USING THE WSR-88D TO FORECAST DOWNBURST WINDS AT CAPE CANAVERAL AIR STATION AND THE KENNEDY SPACE CENTER (CCAS/KSC)

5. FUNDING NUMBERS
None

6. AUTHOR(S)
Gerald David Sullivan, Jr., First Lieutenant, USAF

7. PERFORMING ORGANIZATION NAME(S) AND ADDRESS(ES)
AFIT/ENP
2950 P Street, Building 640
Wright-Patterson AFB, OH 45433

8. PERFORMING ORGANIZATION REPORT NUMBER
AFIT/GM/ENP/99M-12

9. SPONSORING/MONITORING AGENCY NAME(S) AND ADDRESS(ES)
Mr. William P. Roeder (407) 853-8410
45 WS/SYR
1201 Minuteman Street
Patrick AFB, FL 32925-3238

10. SPONSORING/MONITORING AGENCY REPORT NUMBER

11. SUPPLEMENTARY NOTES
Lt Col Michael K. Walters ENP Michael.Walters@afit.af.mil (937) 255-3636

12a. DISTRIBUTION AVAILABILITY STATEMENT
Approved for public release; distribution unlimited

12b. DISTRIBUTION CODE

13. ABSTRACT *(Maximum 200 words)*

The 45 Weather Squadron is tasked with providing several convective wind warnings in support of the U. S. Space Program. The forecasters use a radar-based forecast technique to determine if a thunderstorm has the potential to produce a gust that meets warning criteria. This technique, the Echo Top/Vertically Integrated Liquid Wind Gust Potential (ET/VIL WGP), has not previously been evaluated for use in the Cape Canaveral Air Station and Kennedy Space Center (CCAS/KSC) locale. Additionally, there are two other radar-based forecast techniques that required evaluation for possible inclusion into the 45 WS forecast process. These are the Maximum Reflectivity/ Height of Maximum Reflectivity (d/H) Wind Gust Potential and the Storm Top/Vertically Integrated Liquid (ST/VIL) Wind Gust Potential techniques. Radar data from 15 pulse-type storms that occurred in the CCAS/KSC locale were collected. Potential wind gust forecasts were calculated using the techniques mentioned above. The forecast and observed wind gusts were analyzed using visual and numerical tools to assess the performance of the WGP techniques. Results of the research indicated that the WGP techniques could not consistently predict the magnitude of the downburst gust. The average errors of the prediction were on the order of 10 knots and were quite variable. Because of the small sample size, these results can not be considered as conclusive; however, they may indicate that these techniques do not display the degree of accuracy required to be used operationally by the 45 WS.

14. SUBJECT TERMS
downbursts, microbursts, WSR-88D, potential wind gusts forecasts, Echo Top, Vertically Integrated Liquid

15. NUMBER OF PAGES
110

16. PRICE CODE

17. SECURITY CLASSIFICATION OF REPORT	18. SECURITY CLASSIFICATION OF THIS PAGE	19. SECURITY CLASSIFICATION OF ABSTRACT	20. LIMITATION OF ABSTRACT
Unclassified	Unclassified	Unclassified	UL